DEVELOPMENT OF A FRET BIOSENSOR TO DETECT THE PATHOGEN *MYCOPLASMA CAPRICOLUM*

A Thesis presented to the Faculty of the Graduate School

University of Missouri-Columbia

In Partial Fulfillment

Of the Requirements for the Degree

Master of Science

By

MICHELLE ANNE WINDSOR KRAMER

Dr. Sheila Grant, Thesis Supervisor

DECEMBER 2005

The undersigned, appointed by the Dean of the Graduate School, have examined the thesis entitled

DEVELOPMENT OF A FRET BIOSENSOR TO DETECT THE PATHOGEN *MYCOPLASMA CAPRICOLUM*

Presented by Michelle Anne Windsor Kramer

A candidate for the degree of Master of Science

And hereby certify that in their opinion it is worthy of acceptance.

Dr. Sheila Grant, Biological Engineering

Dr. Kim Wise, Immunology

Dr. Mark Haidekker, Biological Engineering

ACKNOWLEDGEMENTS

First and foremost, I would like to thank my God, my Lord and Savior.

I would also like to thank my family; my mother, Cathy, my fathers, Walter and David, my brother, Christopher, my step-mother Kira, my in-laws, Nola and Richard and lastly my husband, Gentry. Gentry you were my main source of love, support, and comfort during this time. I LOVE YOU ALL!

I also want to thank my advisor, Dr. Sheila Grant, the best advisor in the whole history of advisors. Her knowledge, her drive, her understanding, and her assistance made this time one of the most enjoyable educational times of my life. I also want to thank Darcy Lichlyter for all of her help in lab; Dr. Kim Wise, for so generously sharing his knowledge, time, and interests; and finally, Mark Foecking, for all of his time, effort, and generosity in sharing his research materials with me.

Lastly, I want to thank all of my friends, both out of, and in lab. My best friends, Darcy Denner and Nicole Brossier, my sorority sisters, you two are the best sisters ever. Also I want to thank Dr.Grant's entire lab group, they made this time so much fun!

TABLE OF CONTENTS

LIST OF EQUATIONS

Equation

LIST OF FIGURES

Figure

LIST OF TABLES

Table

DEVELOPMENT OF A FRET BIOSENSOR TO DETECT THE PATHOGEN *MYCOPLASMA CAPRICOLUM*

Michelle Anne Windsor Kramer

Dr. Sheila Grant, Thesis Supervisor

ABSTRACT

Development of a method to quickly and accurately detect pathogens is a growing concern. Mycoplasmas are a species of bacteria that invade any type of cell and can be linked to many chronic diseases. They are highly adaptable to changing environments which makes this particular pathogen difficult to eliminate. We are developing a novel optical biosensor based on Fluorescence Resonance Energy Transfer (FRET) for fast detection of these pathogens. Three different anti-peptide antibodies, α-pep E, α-pep F_1, and α-pep F_2, were conjugated with Alexa-Fluor-546 dye (donor fluorophore). Then the antibodies were complexed to Protein A (or Protein G) labeled with Alexa Fluor-594 dye (acceptor fluorophore) near the Fc-binding region on the antibodies. This complex was then exposed to two different *M. capricolum* antigenic peptides, pep E and pep F, or the entire *M. capricolum* bacteria. The results showed that when the bacteria or peptide specific for the antibody binds, there was a change in the 3-D conformation of the antibody which caused a non-radiative transfer of energy from the donor to the acceptor. The energy transferred to the acceptor was then released radiatively, increasing its

emission. This change of fluorescence was detected in all three antibodies. However, α-pep F_1 had the most distinct conformational change with a 12% differences in signal when exposed to the specific peptide as opposed to the non-specific peptide. The detection complex that utilized the a-pep F1 antibody and Protein G was immobilized onto an optical fiber to see if there was an increase in sensitivity. Finally, a gold nanoparticle quenching system was immobilized onto an optical fiber to see if the quenching system was more sensitive then the two organic fluorophore detection complex. Our current data illustrated that this novel technique measures conformational changes that occur when antibodies and antigens bind and thus is a viable detection method for mycoplasma pathogens.

Key Words: mycoplasma, FRET, biosensor, antibody, optical fiber

CHAPTER 1

LITERATURE REVIEW

1.1 SENSORS AND BIOSENSORS

The Merriam-Webster Dictionary defines a sensor as a device that responds to a physical stimulus and transmits a resulting impulse. There are three types of common sensors: chemical sensors, physical sensors, and biosensors. Chemical sensors are defined as a device which responds to a particular analyte in a selective way through a chemical reaction and can be used for the qualitative or quantitative determination of the analyte (Catterall, 1997). Physical sensors are concerned with measuring physical quantities such as length, temperature, and pressure. Biosensors are defined as a sub-set of chemical sensors that incorporates a biological sensing element connected to a transducer (Eggins, 2002) or a combination of a biological receptor compound and a physical or physiochemical transducer (Brecht, 1995). This doesn't mean that the biosensor will not detect chemical or inorganic analytes; it only means that the recognition element is biological in nature.

1.1.1 BIOSENSOR RECOGNITION ELEMENTS

A general diagram of a biosensor can be seen in Figure 1.1.

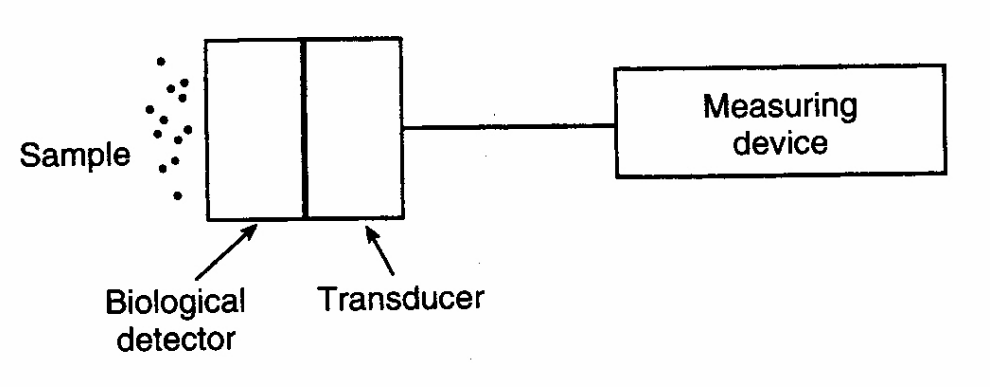

Figure 1.1- Schematic layout of a (bio) sensor showing all of the components (Eggins, 2002)

The biological recognition element is the component of the biosensor that enables the sensor to respond selectively to the analyte. There are four main groups of biological recognition elements: enzymes, antibodies, nucleic acids, and receptors.

An enzyme has an active site to which one or two substrate molecules bind, forming an enzyme-substrate complex. A reaction occurs at the active site, producing an enzyme-product complex. The product is then released, allowing the enzyme to bind additional substrate molecules (Alberts, 2002). This can be seen in Figure 1.2.

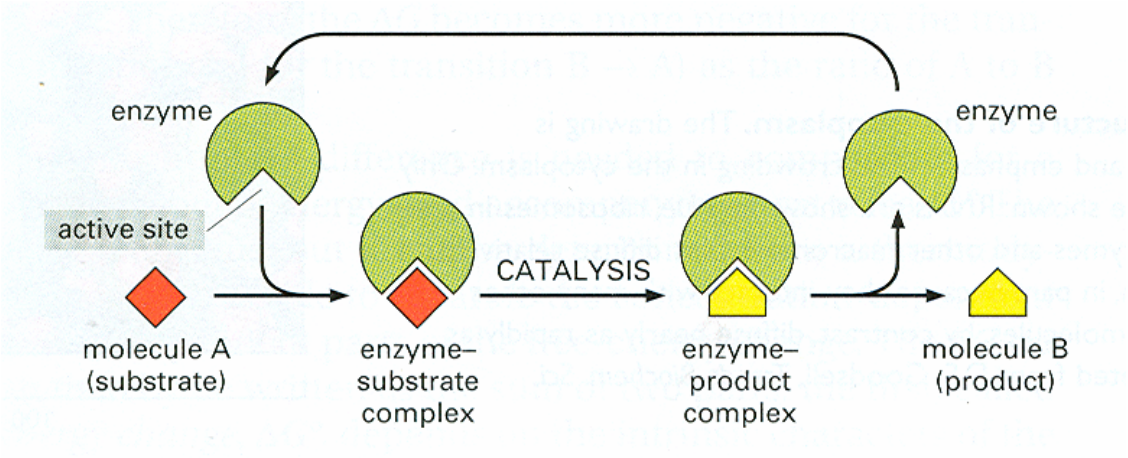

Figure 1.2- A simplified schematic of how enzymes work (Alberts, 2002)

Enzymes are by far the most common of the four types of recognition elements since it has so many advantages. They bind to the substrate, they are highly selective, there is a wide range of enzymes available that are fully characterized, and they have fairly fast acting catalytic activity, which increases the sensitivity of the entire system. However, there are several disadvantages. They are expensive, they tend to deactivate over a short period of time, some enzymes catalyze a range of reactions which hurts the specificity of the desired reaction, and there is a possible loss of activity when immobilized (Eggin, 1997).

One of the most common enzymes used in current research is glucose oxidase. Glucose and oxygen in the presence of glucose oxidase (GOD) catalyzes a reaction that results in the production of gluconic acid and hydrogen peroxide which can be seen in Figure 1.3.

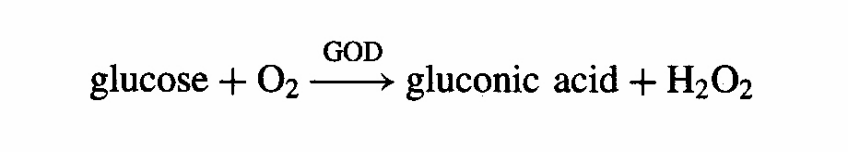

Figure 1.3-Reaction of glucose catalyzed with glucose oxidase (GOD) (Eggins, 2002)

Many methods have been developed to take advantage of all of the benefits that using glucose oxidase as a recognition element entails; including immobilizing GOD on a gelatin film (Sungur, 2004), immobilizing GOD on a nylon net (Maran, 2002), immobilizing GOD on colloidal gold modified carbon paste electrodes (Liu, 2003) and on zeolite enhanced carbon paste electrodes (Serban, 2003). In one instance GOD was trapped within a chitosan-gold nano-particle bio-composite (Luo, 2004). In addition to immobilization, cross-linking GOD inside a matrix with outer layers of membranes that control mass transport (Wagner, 2002) has been tested in brittle diabetic chimpanzees. Also, rat brain glucose levels have been measured with an in vivo micro-sensor that contains an enzyme layer trapped between a layer of cellulose acetate and a layer of polyurethane-MDX4-4210-curing agent for tetrahydrofuran (Hu, 1997).

Antibodies are defined as a type of glycoprotein molecule, also called immunoglobulin (Ig) produced by B lymphocytes that bind antigens, often with a high degree of affinity (Abbas, 2003). The structural features of an antibody can be seen below in Figure 1.4.

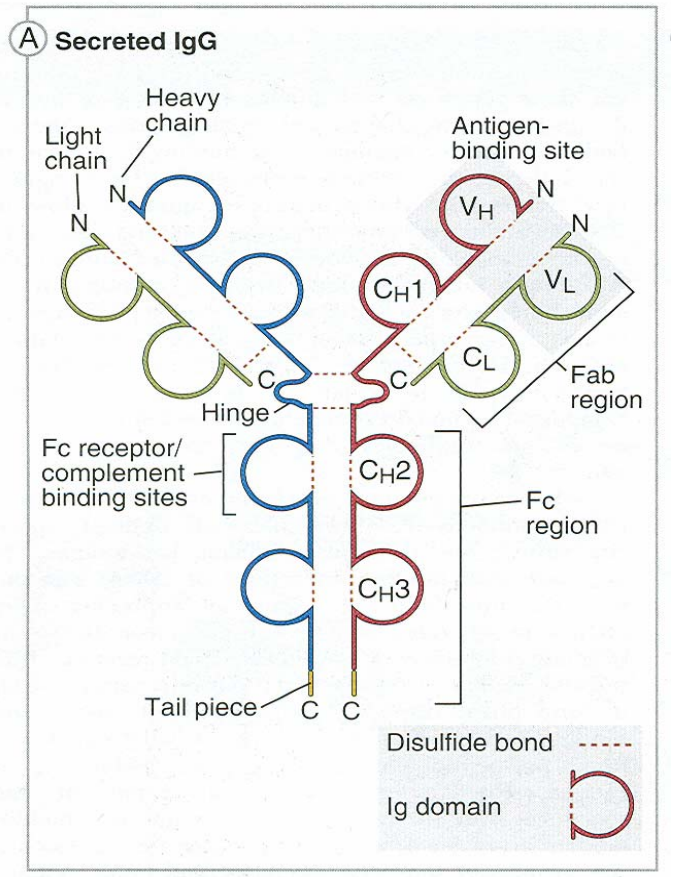

Figure 1.4 – The structure of an antibody molecule, specifically, a secreted IgG molecule (Abbas, 2003)

An antigen is any substance capable of eliciting an adaptive immune response, such as viruses, microbes, and microbial toxins (Alberts, 2002). Using antibodies in biosensors has several advantages. Antibodies are extremely specific and can distinguish between small differences in chemical structures in an antigen which makes them a very powerful selective tool. There are also an extremely large number of diverse antibodies each with a distinct specificity (Abbas, 2003). Antibody proteins can also be produced against most any substance. In addition, they are extremely sensitive and bind very strongly to their

target. Their one main disadvantage is that most lack the catalytic effects that enzymes display (Eggins, 2002).

Utilizing antibodies as the recognition element in sensors has become quite common in the recent past. For example, a multi-analyte array biosensor (MAAB) was used to detect *Salmonella enterica.* In this particular case, various antibodies were immobilized on soda lime glass slides in order to detect multiple analytes simultaneously (Taitt, 2004). In another case, antibodies were immobilized on a surface that consisted of self-assembled mono-layers of thiols on gold (Frederix, 2003). The electrical detection of single viruses was accomplished by antibody immobilization on a silicon nano-wire surface, (Patolsky, 2004). Antibodies have also been key components in the development of biosensors for early detection of myocardial infarction (Pierce, 2004); as well as for the detection of the food-bourne pathogen *Listeria* (Ko, 2003).

Nucleic acids are either DNA or RNA macromolecules consisting of a chain of nucleotides joined together by phosphodiester bonds (Alberts, 2002). An example of such can be seen in Figure 1.5.

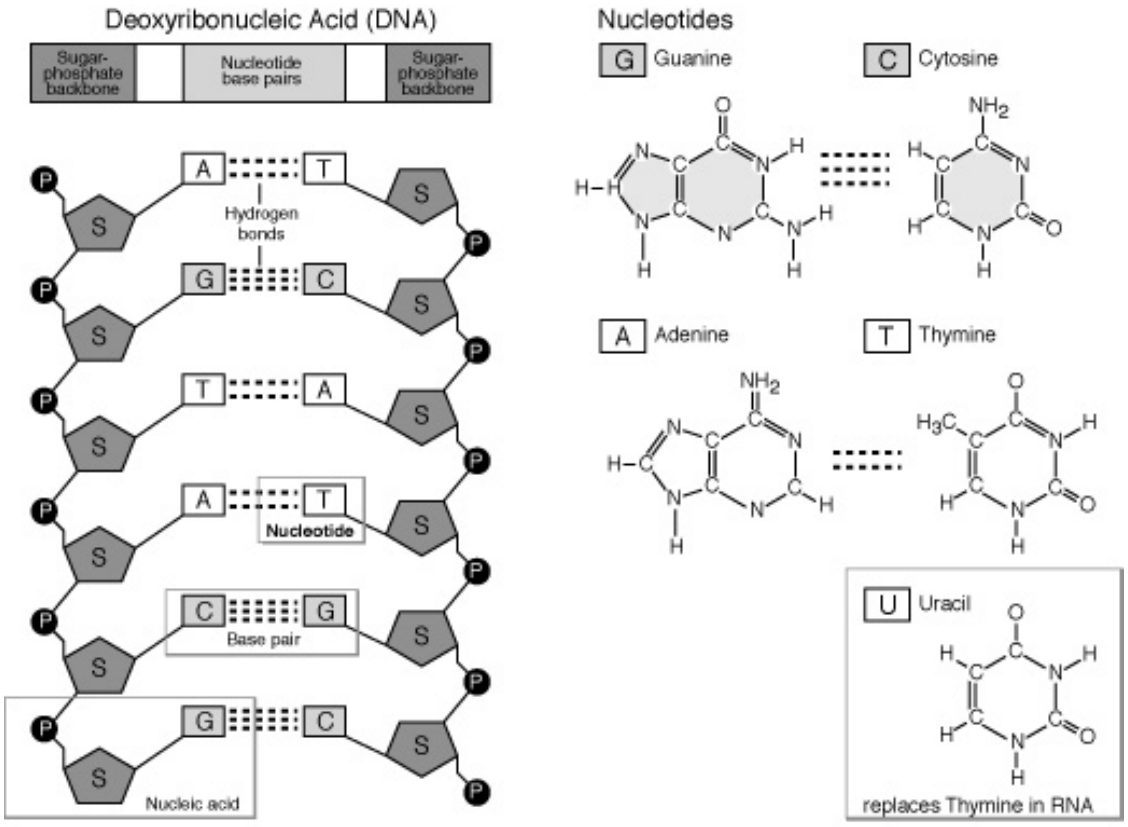

Figure 1.5- A schematic of base-paired nucleic acids

(http://www.accessexcellence.org/RC/VL/GG/nucleotide2.html)

They are rapidly becoming of greater importance of bio-selective agents due to the rapid expansion of knowledge of the structures and roles of genes in biological systems and the recent advances in the technology of their manipulation (Eggins, 2002). Nucleic acids can be synthesized in a very short time and are also available as single stranded molecules. Every desired base sequence can be chosen for synthesis (Abel, 1996). When functioning as DNA probes they can be used to detect genetic diseases, cancers, and viral infections (Eggins, 2002), (Olson, 2004), and (Watzinger, 2004).

Sensors utilizing nucleic acids as the recognition elements have the benefit of forming a complementary sequence with the target. This means that those double strands can be dissociated by heating or by chemical treatments which shows that these sensors are able to be reused multiple times. This can be seen in the immobilization of biotinylated capture probes on an optical fiber surface where they were able to reuse the same fiber for more than 200 cycles (Abel, 1996). The immobilization of a DNA probe specific for a specialized sequence present in genetically modified organisms (Mannelli, 2003) demonstrates the specificity of such a sensor.

Receptors are proteins that bind specific extra-cellular signal molecules and initiate a response in the cell (Alberts, 2002). An example of a hormone receptor can be seen below in Figure 1.6.

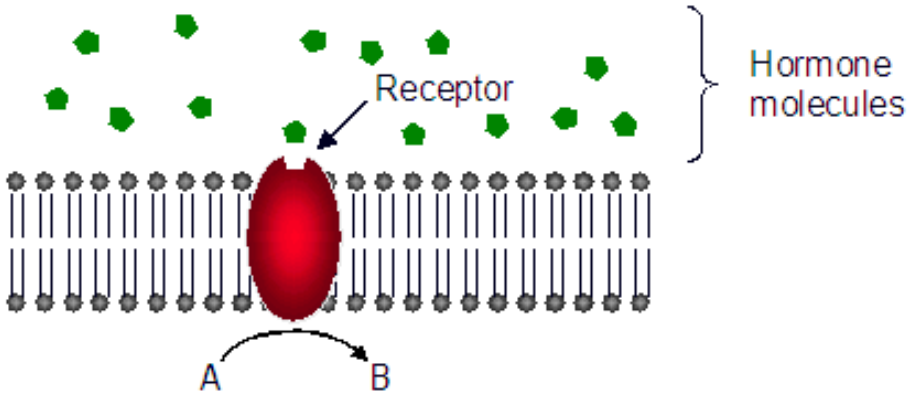

Figure 1.6- The binding of a hormone molecule to a receptor. This initiates a chemical change within the cell. In the diagram above, the binding of hormone and the receptor initiates the conversion of chemical A to chemical B.

(http://faculty.clintoncc.suny.edu/faculty/Michael.Gregory/default.htm)

Most receptors have an affinity for a range of structurally related compounds, rather than one specific analyte and they act as messengers which transmit signals between different parts of a biological system. These types of sensors can be used to study the mechanisms governing the sensitivity, specificity, and regulation of the initiation of cell signaling. A biosensor utilizing total internal reflection illumination and fluorescence correlation spectroscopy has been shown to be able to measure ligand-receptor kinetic dissociation rate constants (Lieto, 2003). However, there is much research yet to do on receptors before they can be commonly utilized in biosensors (Eggins, 2002).

1.1.2 BIOSENSOR TRANSDUCERS

Transduction elements are another crucial part of a biosensor. Transducers are devices that convert an observed change into a measurable signal. They can be subdivided into the following four main types; electro-chemical, optical, piezo-electric devices, and thermal sensors (Eggins, 2002).

Most sensors have been developed around electrochemical transducers because of the simplicity of construction and cost. There are four categories of electrochemical transducers; potentiometric, voltammetric, conductometric, and FET-based sensors.

Potentiometic transducers are based on measuring the potential of a cell at zero current. Voltammetric transducers involve an increasing (or decreasing) potential applied to the cell until oxidation (reduction) of the substance to be analyzed occurs and there is a sharp rise (fall) in the current to give a peak current. The height of the peak current is directly

proportional to the concentration of the electro-active material. If the appropriate oxidation (reduction) potential is known, one may step the potential directly to that value and observe the current. This is called the amperometric mode of voltammetry. A conductometric transducer detects a change in electrical conductivity of the solution after a chemical reaction changes the composition of the solution. Finally, FET (field effect transistor)-based sensors involve miniaturization of any of the types of electro-chemical transducers on a silicon-chip-based FET (Eggins, 2002).

Another popular transducer system is photometric. There are many advantages in the use of optical transducers. For instance, there is no need for a reference electrode, there are no electrical interferences or safety hazards, and an immobilized reagent does not have to be in contact with any optical fibers. In addition, they are highly stable with respect to calibration, they can respond simultaneously to more than one analyte by using multiple immobilized reagents with different wavelengths for response, and they have a higher potential for higher-information content than electrical transducers. However, there are some disadvantages. They will only work if appropriate reagent phases can be developed, they are subject to background ambient light interferences, and they are extensive devices. There are also problems with the long term stability, response times may be slow due to mass transfer, and they have a limited dynamic range when compared to electrical sensors (Eggins, 2002).

Many techniques have been developed to utilize optical transducers, including; absorption spectroscopy, fluorescence spectroscopy, luminescence spectroscopy, internal

reflection spectroscopy, surface plasmon spectroscopy and light scattering (Eggins, 2002). The use of transducers as probes to provide information on the structure and function of bio-sensing layers, and their relation to the transducer surface is becoming a field of importance (Brecht, 1995).

The development of optical fibers has pushed optical transducers to the forefront of current research. Optical fibers behave as waveguides for light, which indicates that the light waves are propagated along the fiber by total internal reflection (TIR). This can be seen in Figure 1.7 and further discussed in Figure 1.19. Optical fibers allow greater flexibility and miniaturization than the older photometric assays.

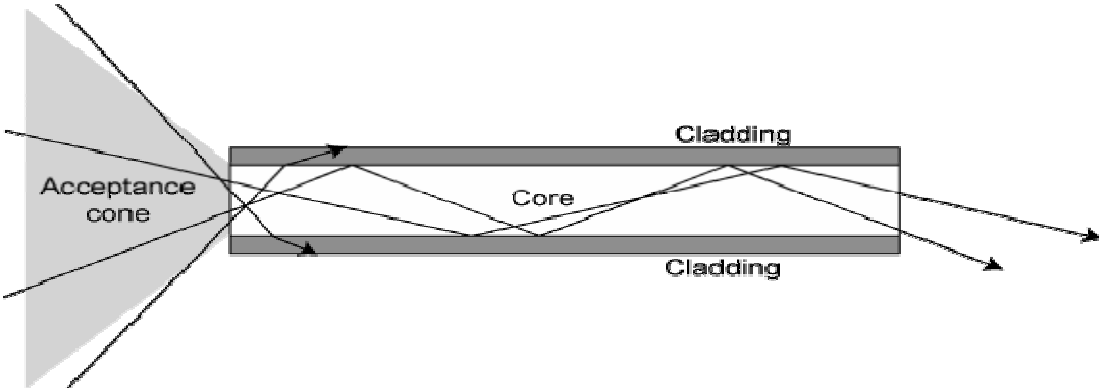

Figure 1.7- Diagram showing how light is guided through an optical fiber (http://www.nationmaster.com/encyclopedia/Image:Optical_fibre.png)

Optical assays have been developed for glucose based on luminescence decay time of the long wavelength dye Cy5™ (Tolosa, 1997). Liquid-core/liquid-cladding optical waveguides have been studied in order to better describe the manipulation of light

(Wolfe, 2004). Optical transducers have also been used to monitor dissolved oxygen inside live cells by organically modified silicate fluorescent nano-sensors in real-time (Koo, 2004).

Piezo-electric devices involve the generation of electric currents from a vibrating crystal. An example of a typical arrangement used in a piezo-electric sensor device can be seen in Figure 1.8.

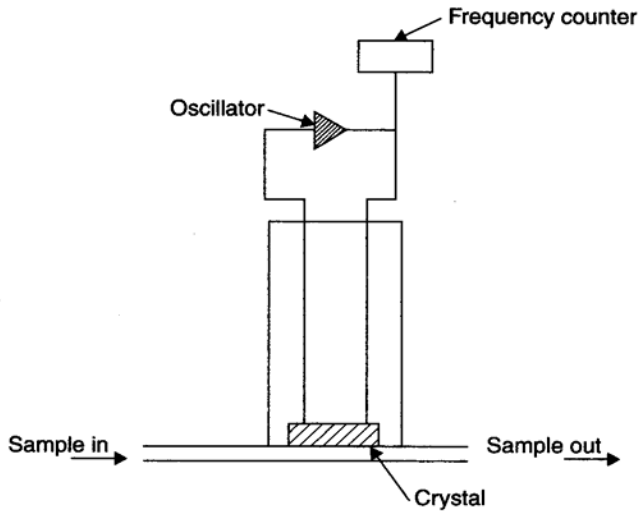

Figure 1.8—A schematic of a typical piezo-electric sensor device (Eggins, 2002)

The mass of material adsorbed on the surface affects the frequency of the vibration (of course, this could be related to changes in a reaction). Surface acoustic wave (SAW) devices are closely related. In SAW's the velocity of the acoustic wave is changed when the wave propagates through or on the surface of the crystal and the sensor measures the change in velocity by measuring the frequency of the sensor (Eggins, 2002).

Heat is either absorbed or produced in all chemical and biochemical processes. This production or absorption of heat can be measured by thermistors in thermal sensors. A schematic of a typical thermistor device can be seen in Figure 1.9.

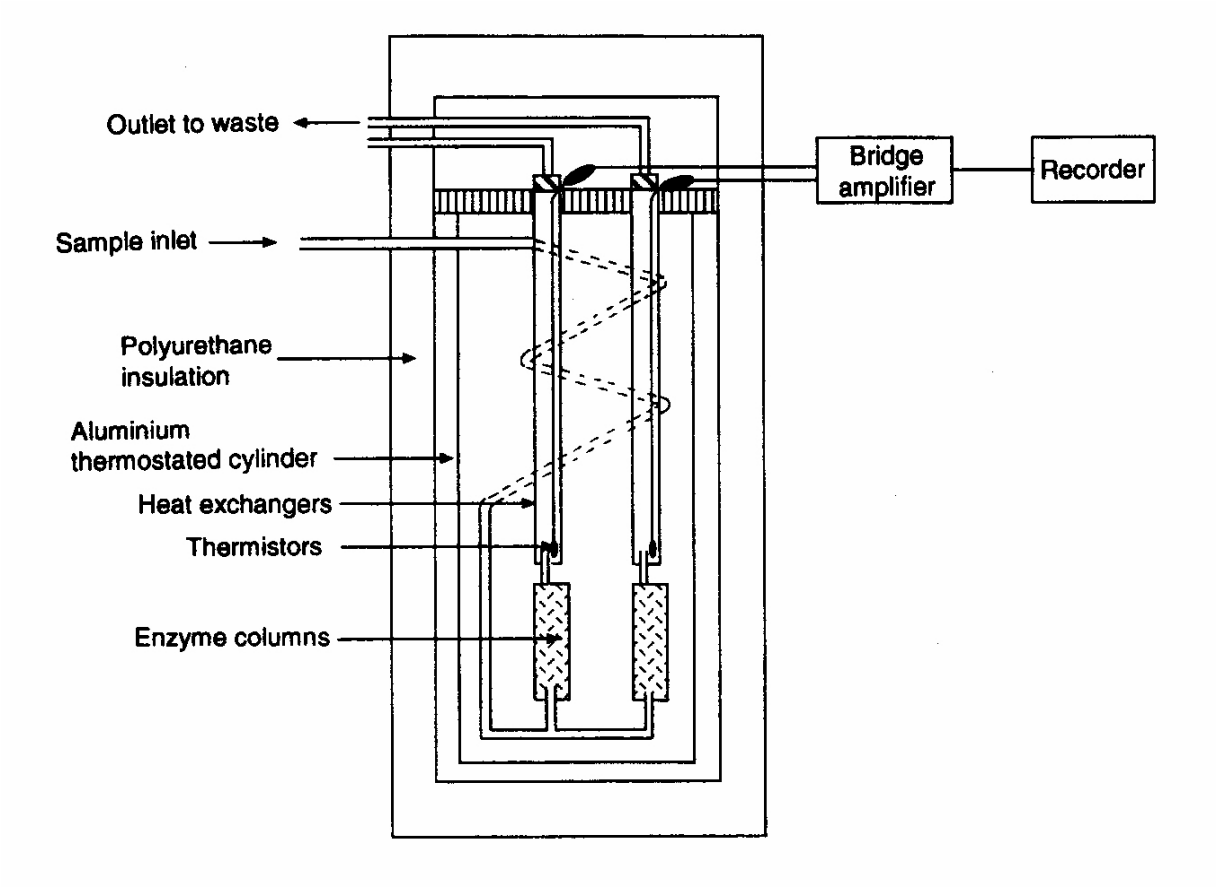

Figure 1.9—A schematic of a typical thermistor device, as used as a biosensor in enzymatic reactions (Eggins, 2002)

This particular measurement can be related to the amount of substance to be analyzed (Eggins, 2002).

1.2 METHODS OF IMMOBILIZATION

The recognition elements must be connected to the transducer in order to have a viable biosensor. Special consideration must be given to immobilizing biological elements so that they retain their functionality. The simplest method is adsorption on to a surface. Micro-encapsulation, one of the earliest methods employed, is simply trapping the sensing element between membranes to ensure close proximity to the transducer. Entrapment is a popular method in which the selective element is trapped within a matrix of a gel, paste, or polymer. Covalent attachment is when covalent chemical bonds are formed between the selective element and the transducer. Finally, cross-linking is when a bi-functional agent is used to chemically bond the selective component to the transducer. Cross-linking is often used with the other methods mentioned above (Eggins, 2002).

1.2.1 ADSORPTION

Adsorption can be divided up into two forms; physical adsorption and chemical adsorption. Physisorption involves the formation of van der Waals bonds, occasionally including hydrogen bonding or charge-transfer forces while chemisorption involves the much stronger covalent bonds. The Langmuir adsorption isotherm is the most generally used model to describe adsorption. It is derived from the kinetics and it relates the fraction of the surface covered by the absorbent (Θ) with the various kinetic parameters seen in Equations 1.1, 1.2, and 1.3 (Eggins, 2002).

Rate of Adsorption = $k_a p_a N(1-\Theta)$ Eqn 1.1

Rate of Desorption = $k_d N\Theta$ Eqn 1.2

$\Theta = Kp_a / (1+Kp_a)$ Eqn 1.3

Equations 1.1, 1.2, and 1.3—Kinetic parameters of adsorption (Eggins, 2002)

At equilibrium Equation 1.1 and 1.2 are equal which then gives up Equation 1.3. K is equal to k_a/k_d where k_a is the rate constant for adsorption and k_d is the rate constant for desorption and p_a is defined as the pressure of the absorbent (Eggins, 2002).

Biomolecules that are absorbed onto a surface are very susceptible to changes in pH, temperature, substrate material, and ionic strength. The typical lifetime for a biosensor using adsorption as the primary immobilization method is approximately one day. (Eggins, 2002)

1.2.2 MICRO-ENCAPSULATION

In this particular method, an inert membrane is used to trap the biomaterial onto or near the transducer. This method has several distinct advantages. It is very adaptable, reliable, and very stable towards changes in temperature, pH, ionic strength, and chemical composition. Its lifetime is approximately one week as opposed to the one day of sensors utilizing the adsorption method of immobilization. This method also has the ability to act as an inbuilt device to limit contamination and biodegradation (Eggins, 2002).

However, some of the membranes used in this method are permeable to small molecule, gases, and electrons. In other words, one must be careful in selecting the correct type of membrane for the desired analyte. For example, a cellulose acetate membrane excludes proteins and slows the transportation of ascorbate which is desired for dialysis (Eggins, 2002).

1.2.3 ENTRAPMENT

In this method, the biological selective agent is added to a polymeric gel solution so that the material is physically trapped in the forming matrix. Unfortunately, this causes barriers to the diffusion of the analyte to the selective agent which slows the response time of the sensor (Eggins, 2002).

Polyacrylamide is the most common gel used for entrapment. Others materials used include starch gels, nylon, silastic gels and conducting polymers (polypyrrole, for example). These materials enhance the lifetime of the sensor by several weeks over that of micro-encapsulation (Eggins, 2002). Methods involving deposition of biomolecule-containing films induced by changing the pH of the solution (Kurzawa, 2002) and electro-deposition (Luo, 2004) have become more common in the past few years.

1.2.4 COVALENT ATTACHMENT

Covalent bonding involves bonding between a non-essential functional group in the biomaterial and the support matrix. These non-essential functional groups used for

coupling are nucleophillic groups such as NH_2, CO_2H, OH, C_6H_4OH and SH. An example can be seen in Figure 1.10 below (Eggins, 2002).

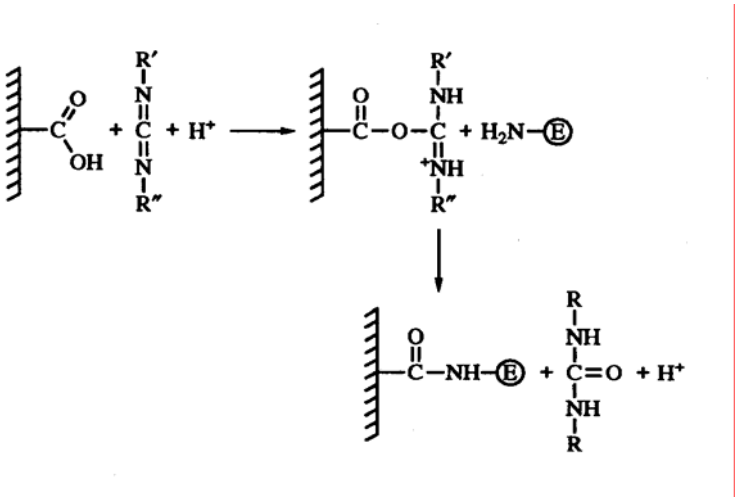

Figure 1.10--Covalent bonding of an enzyme to a transducer by a carbodiimide (Eggins, 2002)

This method's main advantage is because the enzyme will not be released during use, and it has an extended lifetime of 4-14 months (Eggins, 2002). An example of this type of immobilization is using thiol to immobilize haptens containing a carboxyl group to the surface of a sensor (Schlecht, 2002).

1.2.5 CROSS-LINKING

This method of immobilization involves the chemical bonding of the biomaterial to solid supports or to another supporting material (such as a gel) through bi-functional agents.

This method has proved the most useful for stabilizing adsorbed enzymes and other biomaterials. However, there are several disadvantages. Damage is caused to the enzyme, the diffusion of the analyte is limited and there it lacks in mechanical strength. Several examples of cross-linking can be seen in Figure 1.11 (Eggins, 2002).

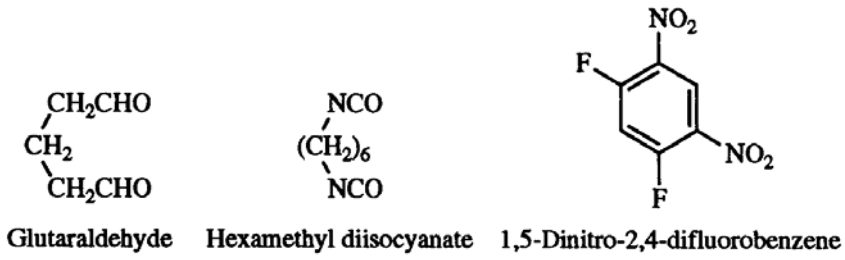

Figure 1.11 –Some common cross-linkers (Eggins, 2002)

This method is rapidly becoming one of the most commonly used due to its stability. It has been used in immobilizing antibodies to substrates ((Ko, 2003), (Sapsford, 2002), and (Pierce, 2004)).

1.3 PRINCIPLES OF FLUORESCENCE

Luminescence is the emission of light from any substance and occurs from electronically excited states. Luminescence is formally divided into two categories, fluorescence and phosphorescence, depending on the nature of the excited state. In excited singlet states, the electron in the excited orbital is paired (of opposite spin) to the second electron in the ground-state orbital. The return to the ground state is spin-allowed and occurs rapidly by emission of a photon. Fluorescence tends to display sub-nano-second lifetimes (Lakowicz, 1999).

Phosphorescence is emission of light from triplet excited states, in which the electron in the excited orbital has the same spin orientation as the ground-state electron. Transitions to the ground state are forbidden and the emission rates are slow, so that phosphorescence lifetimes are typically milliseconds to seconds (Lakowicz, 1999).

1.3.1 JABLONSKI DIAGRAM

Jablonski diagrams are often used as the starting point for discussing light absorption and emission. These diagrams illustrate the processes which occur between the absorption and emission of light. An example can be seen in Figure 1.12 below.

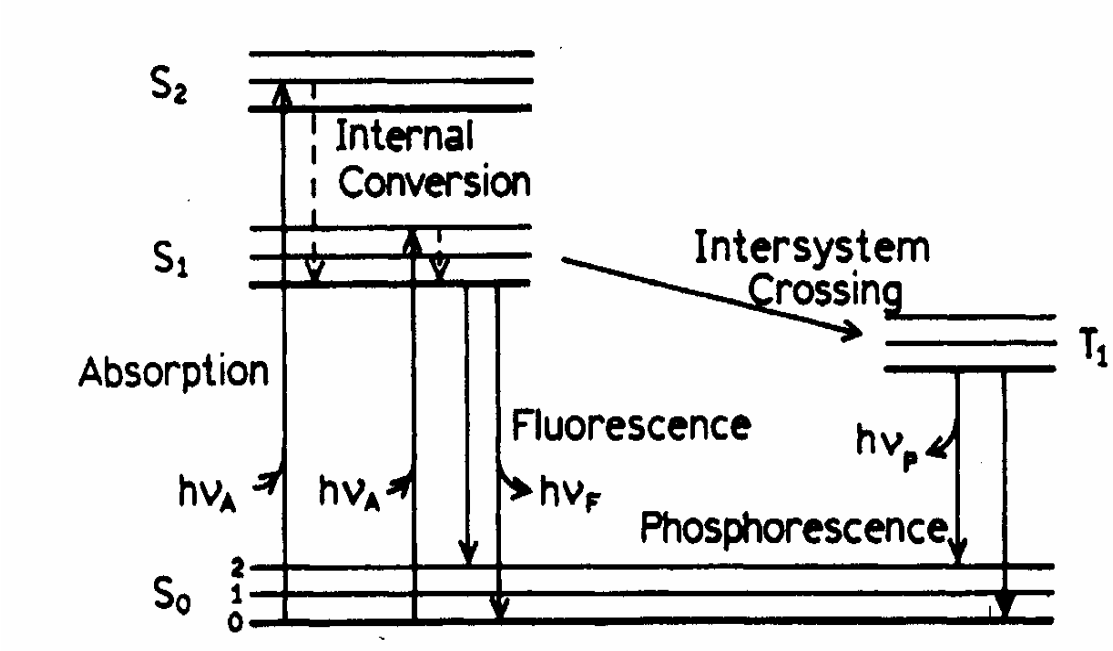

Figure 1.12— One form of a Jablonski Diagram (Lakowicz, 1999)

The singlet ground (S_0), first (S_1), and second (S_2) are electronics states that can be seen in Figure 1.12 above. At each of these electronic energy levels the fluorophores can exist in a number of vibrational energy levels, which are denoted as 0, 1, 2, etc. Absorption typically occurs from molecules with the lowest vibrational energy. The larger energy difference between the S_0 and S_1 excited states is too large for the thermal population of S_1 (that is the reason that light is used instead of heat to induce fluorescence) (Lakowicz, 1999).

Following light absorption, several processes usually occur. A fluorophore is usually excited to some higher vibrational level of either S_1 or S_2. Molecules in the condensed phases rapidly relax to the lowest vibrational level of S_1; this is called internal conversion (IC). This occurs more rapidly than does fluorescence, so IC occurs before emission. Fluorescence emission generally results from the lowest-energy vibrational state of S_1 (Lakowicz, 1999).

Return of the ground state typically occurs to a higher excited vibrational ground-state level which then quickly reaches thermal equilibrium. This results in a phenomenon that is known as the mirror image rule. This is when the emission spectrum is a mirror image of the absorption spectrum of the S_0 to S_1 transition. This occurs because the electronic excitation does not greatly alter the nuclear geometry. The spacing of the vibrational energy levels of the excited state is similar to that of the ground state which results in similar vibrational structures seen in the absorption spectra and the emission spectra (Lakowicz, 1999).

Molecules in the S1 state can also undergo a spin conversion to the first triplet state T1. Emission from this state is termed phosphorescence and is generally shifted to longer and longer wavelengths (lower energy) relative to the fluorescence. Conversion of S1 to the first triplet state is called intersystem crossing (ISC). Transition from T1 to the singlet ground state is forbidden, so the rate constants for triplet emission are several orders of magnitude smaller than those for fluorescence (Lakowicz, 1999).

1.3.2 FLUOROPHORES

Fluorophores are defined as a fluorescent substance. They are divided into two general classes: intrinsic or extrinsic. Intrinsic fluorophores are those that occur naturally. This includes three amino acids (tryptophan, tyrosine, and phenylalanine), and some enzyme cofactors (NADH, FAD, pyridoxal phosphate, and pyridoxamine phosphate, riboflavin, and FMN) (Lakowicz, 1999).

Extrinsic fluorophores are those that are added in order to force a sample to display the desired spectral properties. Usually, these fluorophores are used to label proteins so that they can be studied in the presence of other unlabeled proteins. In the past several years, the number of fluorophores has increased drastically so that they now cover a wide range of spectral properties (Lakowicz, 1999). Molecular Probes, a member of the Invitrogen Corporation, has a wide selection of fluorophores just for labeling proteins. Quantum dots (QD) are a type of fluorescent semiconductor nanocrystals that can be used for ultra-sensitive biological detection. Compared to organic dyes, these highly luminescent semi-

conducting nanocrystals are 20 times brighter and 100 times as stable against photo-bleaching (Chan, 1998). QDs have been used to provide real-time visualization of draining lymphatic channels and nodes (Soltesz, 2004) and as probes for transmission electron microscopy (TEM) (Nisman, 2004). Other examples can be seen in Figure 1.13 below.

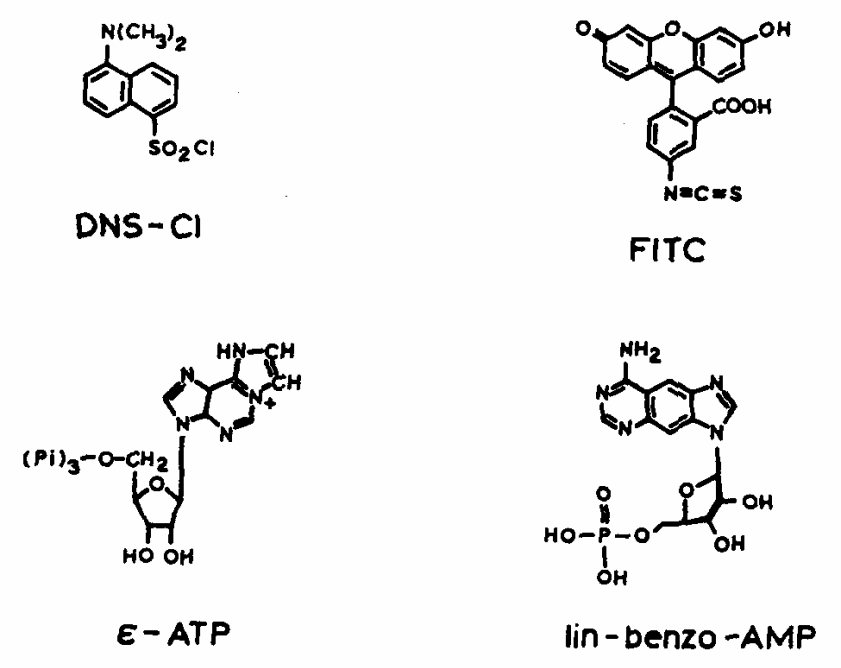

Figure 1.13– Examples of some fluorophores for covalent labeling (DNS-CI and FITC) and fluorescent nucleotide analogs (ε-ATP and *lin*-benzo-AMP) (Lakowicz, 1999)

1.3.3 FLUORESCENCE RESONANCE ENERGY TRANSFER (FRET)

FRET stands for Fluorescence Resonance Energy Transfer. It is a transfer of the excited-state from the initially excited donor fluorophore (D) to an acceptor fluorophore (A). In

order for the transfer of energy to occur between two fluorophores, the fluorescence spectra of the donor fluorophore must overlap the absorption spectra of the acceptor fluorophore as seen in Figure 1.14.

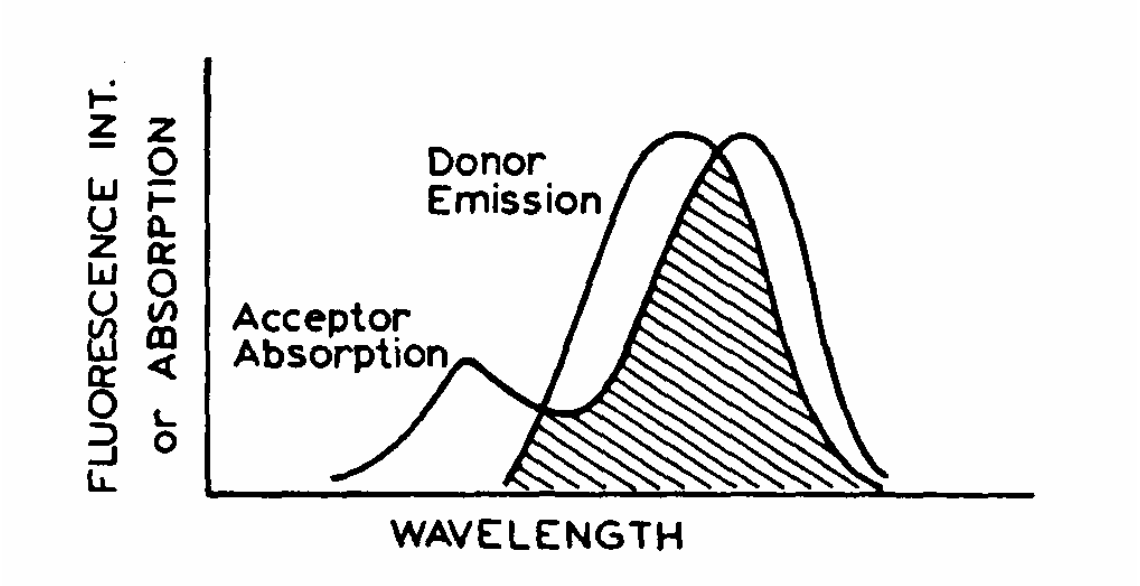

Figure 1.14– Fluorescent intensity or Absorption versus the wavelength for the emission of the donor and the absorption of the acceptor. Take note that the donor emission spectra overlap the acceptor absorption spectra (Lakowicz, 1999)

Förster's distance is defined as the distance at which the efficiency of energy transfer is 50%. When the two fluorophores are within Förster's distance (Trp and DNS in Figure 1.15), excited-state energy is transferred non-radiatively (without emission of a photon) from the donor to the acceptor. This phenomenon causes a decrease in the fluorescence intensity of the donor and an increase in the fluorescence intensity of the acceptor. This can be seen in Fig 1.15. The right axis is the molar extinction coefficient which is the

absorbance for a molar concentration of a substance with a path length of l cm determined at a specific wavelength.

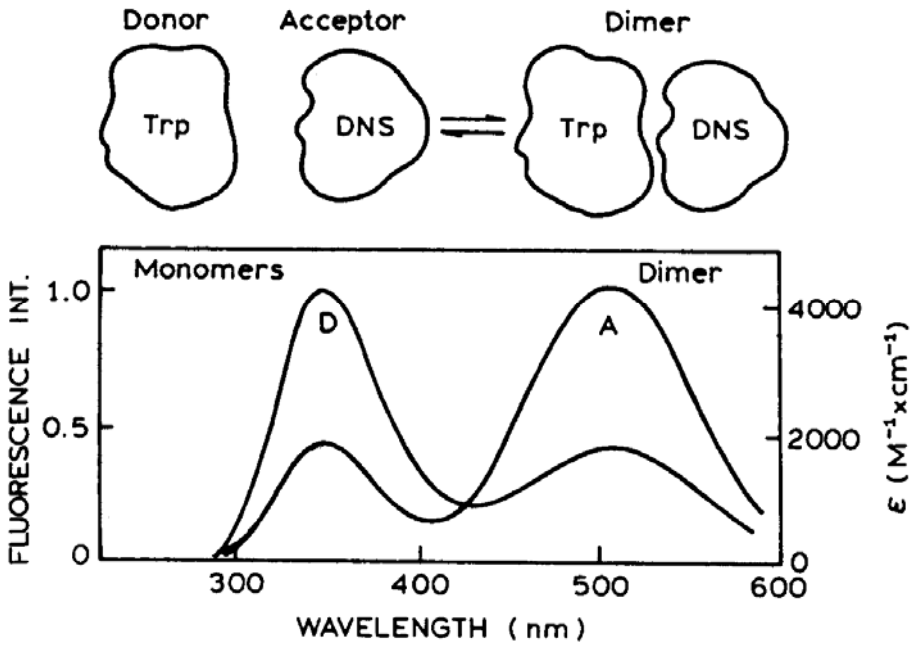

Figure 1.15 –Example of FRET (Lakowicz, 1999)

The rate of energy transfer depends upon several factors: the quantum yield of the donor, the relative orientation of the donor to the acceptor transition dipoles, and the distance between the donor and acceptor molecules. The efficiency of the energy transfer is the fraction of the photons absorbed by the donor that are transferred to the acceptor. The efficiency is strongly dependant upon distance when near Forster's distance. It increases to 100% as the distance between the donor and acceptor decreases below the Forster's distance.

$$E = \frac{R_0^6}{R_0^6 + r^6}$$

Equation 1.4– The equation that relates the efficiency of energy transfer with the Forster's Distance when the donor and acceptor fluorophores are at a fixed distance (Lakowicz, 1999)

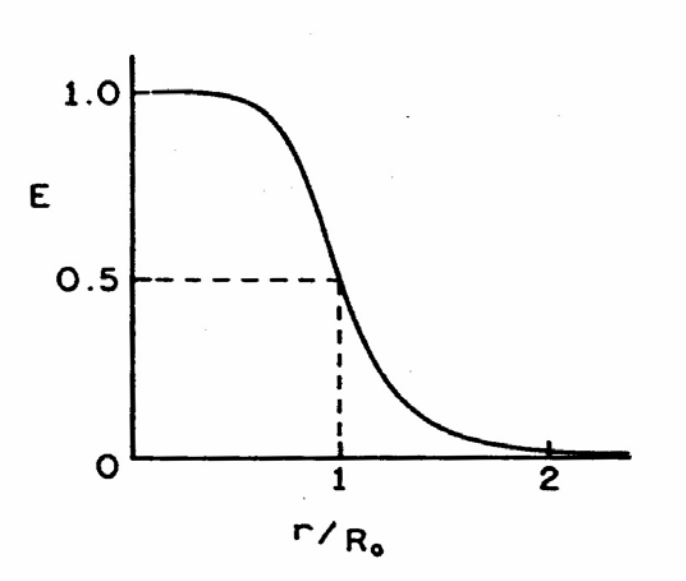

Figure 1.16-- The graphical representation of Equation 1.4 (Lakowicz, 1999)

The FRET phenomenon has many applications, but in particular, it has the ability to detect conformational changes among proteins (Mekler, 1997). FRET techniques have been used to detect various antibodies, (Lichlyter, 2003), bacteria (Ko, 2003), sugars (Medintz, 2003), and to elucidate complex interactions between molecules associated with cancerogenesis (Schmid, 2003).

1.3.4 QUENCHING

Quenching is defined as a process that causes a decrease in the intensity of fluorescence. There are two main types of quenching; static and dynamic. Static quenching occurs before the excitation of the fluorophore while dynamic quenching occurs during the excitation of the fluorophore. In some instances, a fluorophore can be quenched by both static and dynamic quenching. Quenching can be cause by molecular oxygen, aromatic and aliphatic amines, and heavy atoms such as iodine and bromine (Lakowicz, 1999). Other examples can be seen in Figure 1.17 below.

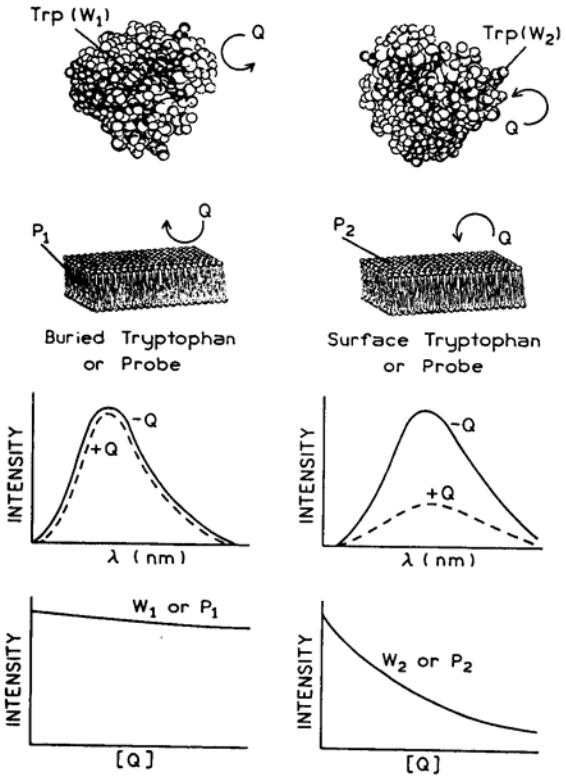

Figure 1.17— Example of how the accessibility of a fluorophore varies in response to a quencher (Q-) (Lakowicz, 1999)

In static quenching, a non-fluorescent, weakly bound complex is formed by the quencher and the fluorophore while at the ground state. When this complex absorbs light, it immediately returns to the ground state without emission of a photon. However, if there is any unbound fluorophore in the solution it will remain unquenched unless bound by the quencher (Lakowicz, 1999).

For dynamic (or collisional) quenching, the quencher diffuses into the fluorophore during the lifetime of the excited state. When the fluorophore and the quencher come into contact, the fluorophore returns to ground state without emitting a photon. This type of quenching can be described by the Stern-Volmer Equation in Equation 1.5(Lakowicz, 1999).

$$\frac{F_0}{F} = 1 + k_q \tau_0 [Q] = 1 + K_D [Q]$$

Equation 1.5— Equation for Dynamic Quenching (Lakowicz, 1999)

In static quenching, a non-fluorescent, weakly bound complex is formed by the quencher and the fluorophore while at the ground state. When this complex absorbs light, it immediately returns to the ground state without emission of a photon. However, if there is any unbound fluorophore in the solution it will remain unquenched unless bound by the quencher (Lakowicz, 1999). Static quenching can also be described by the Stern-Volmer equation with a static quenching constant. This can be seen below in Equation 1.6.

$$\frac{F_0}{F} = 1 + K_S[Q]$$

Equation 1.6– Equation for Static Quenching (Lakowicz, 1999)

In some instances, a fluorophore can be quenched by both static and dynamic quenching. Quenching can be used at any point in a system. For example, a quantum dot (donor fluorophore)-maltose binding protein (MBP) - B-cyclodextrin (an acceptor dye)-QSY9 (dark quencher) can be assembled in order to quench the emission of the quantum dot. The quencher (QSY9) can be displaced by maltose (the analyte of interest) which causes an increase in the fluorescence of the quantum dot (Medintz, 2003). Gold nanoparticles can also act as a quencher of fluorescence with high efficiency (Dubertret, 2001), (Dulkeith, 2002), and (Fan, 2003).

1.4 FIBER OPTIC BIOSENSORS

The use of fiber optics is growing in many fields such as optical instrumentation, communication, and laser beam delivery for surgical and other important applications. An optical fiber consists of a core, cladding, and a jacket. The core can be either plastic or glass, but glass is optimal for minimal losses. The cladding consists of a paper thin polymer which has a lower index of refraction than the core. The jacket usually consists of Teflon (Grant, 2005).

There are several different types of fibers depending on how the fibers are made and the type of cladding used. The single mode fiber is used for communication purposes such as in a submarine cable system. It requires a laser source, has a very large bandwidth, a very small core (which leads to difficulties splicing), and is relatively inexpensive. A multimode step index is used for data links, but cannot be used for communication due to modal dispersion. It requires a laser or light emitting diode (LED) as a light source, has a large bandwidth (but not as large as the single mode fiber), is difficult to splice (but doable), and is the least expensive type of optical fiber. Finally, there is a graded index multimode fiber. The refractive index of this fiber decreases radially from the center in a parabolic fashion. An example of an application for this type of fiber would be as a telephone trunk between central offices. This fiber requires a laser or LED, and has a very large bandwidth (still not as large as the single mode fiber), splicing is difficult (but doable), and is the most expensive type of optical fiber (Grant, 2005).

Light is transmitted through a fiber by total internal reflection or TIR. This concept is demonstrated in Figure 1.18 below.

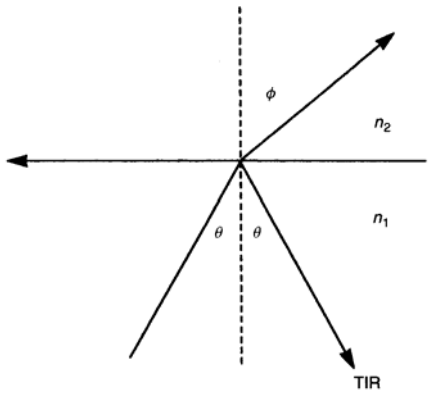

Figure 1.18— Total internal reflection is guided by Snell's Law: $n_1 \sin\Theta_1 = n_2 \sin\Theta_2$

(Rabbany, 1994)

If a fiber core is clad with a material of lower refractive index than the core, there will be a critical angle such that rays striking the interface of the core and cladding at an angle greater than this angle will be totally reflected. The acceptance angle is the greatest possible angle is the greatest possible angle that can be launched into the core and still be guided into the optical waveguide. Thus the fiber becomes a light guide (Grant, 2005). This can be seen in Figure 1.19.

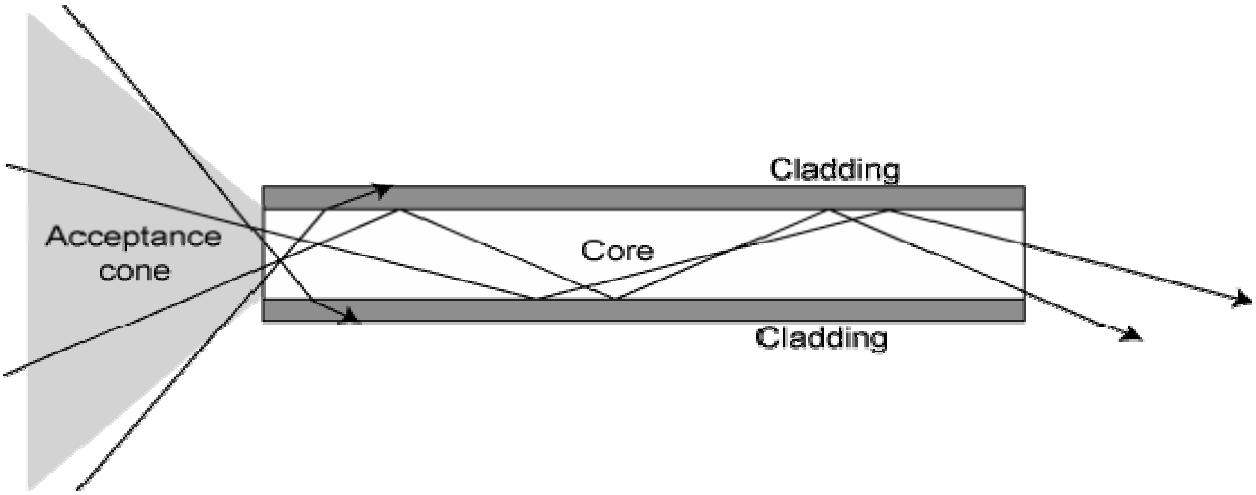

Figure 1.19—The acceptance cone of an optical fiber

(http://www.nationmaster.com/encyclopedia/Image:Optical_fibre.png)

The sine of the acceptance angle is called the numerical aperture. The numerical aperture (NA) is a measure of the light gathering ability of an optical fiber. Typically the NA is between 0.2-0.5. For sensors a high NA is desired. This indicates a larger acceptance angle and thus a better light gathering ability (Grant, 2005).

1.5 EVANESCENT WAVE SENSING

When antibodies are immobilized directly on the external surface of the exposed core, the evanescent wave phenomenon is exploited for signal generation. In preparation for immobilization, the fiber is modified by stripping the cladding (and polymer coating) off the sensing region, cleaning it with acid, and coating it with silanization agents. Then, a cross-linking agent is used to couple the antibody to the silane film. The signal propagation is facilitated by the law of total internal reflection discussed above in Figure 1.19 but only when the angle of incidence is greater than the critical angle. The critical angle is defined in Equation 1.7.

$$\Theta c = \sin^{-1} (n_2/n_1)$$

Equation 1.7 –Critical angle equation (Rabbany, 1994)

The reflected light then propagates in the direction parallel to the fiber. When the light strikes the interface, it undergoes total internal reflection (seen in Figure 1.20) and the electromagnetic component of the light- the evanescent wave-traverses the interface. The evanescent wave propagates through the lower index medium in a direction parallel to the surface of the core before it couples back into the core.

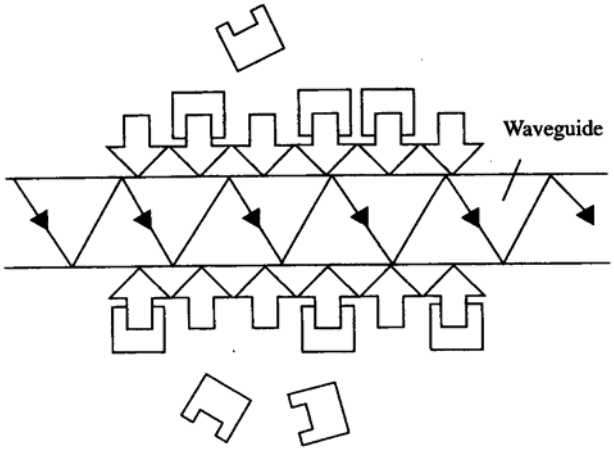

Figure 1.20—TIR on an optical fiber with immobilized reagent binding to its specific analyte (Eggins, 2002)

By stripping the cladding and immobilizing the substrate directly onto the core, the evanescent wave travels through the sensing layer itself and into the sample medium a limited depth which is proportional to the wavelength of light used. This limited depth (or penetration depth) decays exponentially. This makes this system impervious to interfering effects outside of the reaction area (Rabbany, 1994).

Evanescent wave immunosensing can be either direct or indirect. In direct sensing, for example, the antibody can be immobilized on the core and then introduced to its specific analyte. The binding of the analyte alters the spectral properties of the sensing layer, producing a returning signal which is measured. This type of sensing can be achieved by measuring a change in refractive index, visible spectra, or fluorescence. In the case of fluorescence, the fluorescence of the substrate or the analyte can be enhanced or reduced

upon binding. Fluorescently labeled proteins outside of the evanescent field are not excited and their presence does not interfere with the signal (Rabbany, 1994).

Optical biosensor systems have been utilized to detect oligonucleotides in DNA hybridization assays (Abel, 1996). In 2001 evanescent illumination was used to measure the real-time binding kinetics of antigens to immobilized antibodies (Sapsford, 2001). Also, in 2004, a multi-analyte array biosensor used the evanescent wave phenomenon to detect multiple analytes simultaneously (Taitt, 2004). Recent research has lead to advances in the field of optical biosensors, such as tapering the tips of silica core optical fibers. Experiments have been performed that demonstrate tapering of the fiber tip can lead to increases in sensitivity (Ahmed, 2004).

CHAPTER 2

INTRODUCTION

2.1 MYCOPLASMA SPECIES

The mycoplasma genus contains more than 1000 species. They are prokaryotic bacteria that lack a cell wall (class *Mollicutes*) which distinguished them from walled bacteria. They have a circular, double stranded DNA genome. Most mycoplasmas are parasites that are only able to thrive within a narrow range of hosts. This means that species that are natural pathogens of rodents are distinct from species that are natural pathogens of humans. The natural habitats of mycoplasmas include mammals, birds, reptiles, arthropods, plants, and fish (Dybvig, 1996).

Mycoplasmas exhibit several unusual properties. Of all known cellular organisms, mycoplasmas have the smallest reported genomes (in some cases less than 600 kilo-bases). For such successful pathogens the size of their genome is remarkable. Their DNA can undergo rearrangements that reassort coding regions to maximize their limited genomes coding potential. Because of their limited genome, mycoplasmas lack many enzymatic pathways that are characteristic of most bacteria. This means that the organisms are extremely particular in their nutritional requirements. Mycoplasmas produce high levels of degrading enzymes such as nucleases and proteases, and scavenge required nutrients from other, mainly eukaryotic cells (Dybvig, 1996).

In addition, their DNA contains very low amounts of guanine + cytosine. Mycoplasmas also contain repetitive elements that are related to genes that encode important surface antigens. Another unusual prospect of mycoplasmas is their codon usage. TGA, which is a stop codon in most organisms, encodes tryptophan in most mycoplasma species (Dybvig, 1996). Many mycoplasmas require exogenous cholesterol for membrane function and growth (Baseman, 1997), which is fairly unique in prokaryotes (Razin, 1985).

Mycoplasmas can interact with the host cell in different ways. Most mycoplasmas that infect humans and other animals are surface parasites that adhere firmly to the epithelial linings of the respiratory and urogenital tracts (Razin, 1985). Some mycoplasmas have evolved mechanisms for entering host cells. This intracellular environment protects the parasite from the immune system as well as from the action of many antibiotics (Rottem, 2003) and (Citti, 2005). The lack of a cell wall allows direct contact of the mycoplasma to the host cell. Under appropriate conditions, this may lead to cell fusion (Rottem, 2003).

There are several possible mechanisms of damage to host cells. Competition for biosynthetic precursors between the mycoplasmas and the host cell can result in disruption of host cell integrity and alter host cell function. The association between the adhering mycoplasmas and their host cells may interfere with membrane receptors or alter transport mechanisms of the host cell. Also, the host cell is vulnerable to toxic metabolites excreted by the parasite that are able to build up and cause tissue damage.

This includes oxidative damage to the host cell membrane by peroxide and super-oxide radicals. During the fusion process, mycoplasma components are delivered into the host cell and affect the normal functions of the cell. An example of this would be the release of a potent phosphoprotein phosphatase that interferes with the host cells normal signal transduction cascade. In addition, mycoplasmal attachment to eukaryotic cells may sometimes lead to a pronounced cytopathic effect. These effects result in micro-colony formation producing micro-lesions and small foci of necrosis (Rottem, 2003).Overall, pathogenic human and animal mycoplasmas infection results in localized infections and clinical manifestations such as pneumonia, endometritis, or mastis. The ability of mycoplasmas to cycle between the extra-cellular and intra-cellular compartments in their hosts could be a major factor in establishing a persistence infection in immuno-competent hosts (Citti, 2005).

Survival of a mycoplasma within its host depends greatly on its ability to circumvent the host immune system. Two mechanisms used are molecular mimicry and phenotypic plasticity. Molecular mimicry is when the antigenic epitopes shown by mycoplasmas are shared by host cells. Phenotypic plasticity is the ability of a single genotype to change its antigenic makeup producing more than one alternative form of morphology, physiological state, and/or behavior in response to an environmental condition. Phenotypic plasticity is accomplished in two distinct ways: in response to environmental signals or by random changes of expression of single or multiple genes (Rottem, 2003). In addition, many mycoplasmas undergo high-frequency variations in their surface-antigen production. It is commonly proposed that the variations in mycoplasma surface

proteins contribute to disease pathogenesis by allowing the mycoplasma to survive in different niches and/or by enabling the mycoplasma to escape host-defense mechanisms. However, the mechanisms by which they accomplish this antigenic diversity, varies greatly between species (Dybvig, 1996). Nevertheless, the expression of abundant, variable surface antigens that are usually specific for a mycoplasma species, offers a potentially useful target for selective recognition of the organism.

The ability of mycoplasmas to reside, persist, and multiply in cultured animal cells are the primary reason that they are perceived by scientists as nuisances. Their mere presence may compromise or invalidate research data. So, much time and effort has been put forth in order to control and prevent mycoplasma contamination of cell cultures. It is extremely difficult to eradicate contaminating mycoplasmas even with high and prolonged doses of antibiotics (Citti, 2005). Mycoplasmas are resistant to antibiotics that specifically inhibit bacterial cell wall synthesis. However, they are sensitive to tetracyclines, macrolides, and the newer quinolones (Razin, 1985). Improved methods for rapid and selective detection of mycoplasmas in cell culture are still an unfilled need in this area of research.

2.2 DETECTION METHODS

Protein-based or immunological diagnostic techniques are routinely used to identify the species of the infecting mycoplasma. These immunological techniques are mainly based on interaction of antibodies with mycoplasma surface or cytoplasmic antigens. During the last decade, monoclonal antibodies have been increasingly used in a variety of

diagnostic techniques. Some examples include metabolic inhibition, growth inhibition, and immunoblotting assays. Monoclonal antibodies have also been used for specific detection of particular mycoplasma species in clinical samples, and against consistently expressed species-specific epitopes of mycoplasma surface antigens in monoclonal antibody blocking enzyme-linked immunosorbent assays (B-ELISAs) (Markham, 2005) and (Sharew, 2005).

Nucleic acid detection can also be used to indirectly detect mycoplasma infection, by use of DNA-binding fluorochrome dyes specific for mycoplasma DNA. In addition, restriction fragment length polymorphism or RFLP can be used to distinguish between mycoplasma species and strains due to the unique patterns produced by restriction endonuclease digestion of mycoplasma DNA (Razin, 1985), (Markham, 2005). Also, amplified fragment length polymorphism (AFLP) and pulsed field gel electrophoresis (PFGE) fingerprinting techniques have also been used (Kusiluka, 2001). Nucleic acid detection for mycoplasmas also includes polymerase chain reaction systems or PCR (Razin, 1985), (Houshaymi, 2002), (Woubit, 2004), and (Markham, 2005). PCR has the ability to amplify detectable amounts of DNA within a few hours. PCRs sensitivity has proven useful for identifying poorly growing or non-cultivable organisms. A useful target for PCR is the 16S rRNA sequence (the basis for phylogenetic groupings). Multiplex PCRs also have the ability to be able to detect more than one species in a single test. Finally, direct sequencing of cloned mycoplasma DNA is becoming more common (Markham, 2005). Other various types of tests have been used, but mentioned

above are the most commonly used (Ikheloa, 2004), (Wesonga, 2004), and (Al-Momani, 2005).

2.3 *MYCOPLASMA CAPRICOLUM*

Mycoplasma capricolum subsp *capricolum* strain California Kid (ATCC 27343) was used as the basis for these studies and is referred to as "*M. capricolum"* in this document. This organism is an infectious agent of goats and sheep. It is a member of a close phylogenetic group of mycoplasmas termed the "*M. mycoides* cluster" that includes additional mycoplasmal agents of marked pathogenicity. However, although this particular subspecies and strain of *M. capricolum* is distinct from more severe pathogens (such as *M. capricolum* subsp *capripneumoniae,* causing contagious caprine pleuropneumonia), it presents some analogous clinical manifestations. Importantly, it also serves as a critical and versatile model for studying the genetics, biology and immunological aspects of all subspecies within the *M. mycoides* cluster.

M. capricolum expresses a set of abundant surface antigens (Vmc lipoproteins) that is useful to explore as targets for selective diagnostic assays that may be generally applicable to organisms in the *M. mycoides* cluster. Vmc proteins have been described previously (Wise et al 2003). They are subject to high frequency variation in expression, and are structurally organized to present lipid-anchored surface proteins that contain tandemly-repeating amino acid sequences. These repeats are antigenic and surface-binding antibodies (both polyclonal and monoclonal) have been raised in mice. The

genome is 1,010,023 base-pairs, and has a guanine + cytosine content of 23.8%. Repetitive sequences make up approximately 8% of its genome (Wise, 2005).

2.4 RESEARCH OBJECTIVE

The overall objective of this research is to develop a novel FRET immunosensor to detect the caprine pathogen *M. capricolum*. While many advances have been made in biosensor technology, many technological problems remain such as false positives/false negatives, poor specificity, and slow response times. The proposed optical technique offers several advantages over existing techniques. The biosensor may be able to detect a change in fluorescence as a result of a conformational change in the monoclonal antibodies directed to defined epitopes in VmcE and VmcF surface proteins of *M. capricolum*. Since only viable molecules can cause this change, the biosensor will have a very low incident of false positive readings. Additionally, the biosensor will have inherent specificity due to the nature of antibody-antigen bindings.

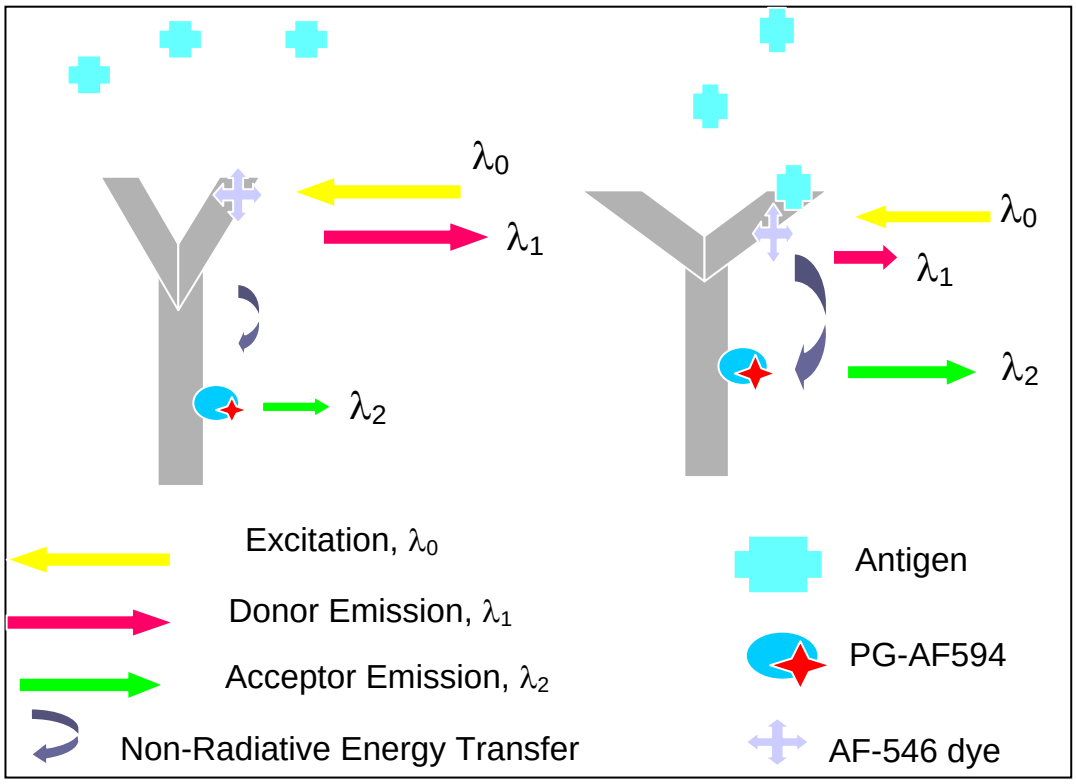

Figure 2.1-Proposed Detection Technique

The proposed technique in Figure 2.1 is single-step detection, unlike the competitive and non competitive binding techniques. There is no incubation or sample preparation needed. The specific aims include:

Specific Aim #1: Develop and test a FRET nanoprobe in to detect *M. capricolum* in solution. The hypothesis is that the antibody would undergo a conformational change when exposed to both the peptide as well as the organism. The FRET nanoprobes utilizes organic fluorophores as the donor and acceptor fluorophores.

Specific Aim #2: Immobilization of the FRET nanoprobes to optical fibers to test the biosensor response. It is hypothesized that immobilization of the nanoprobes would result in a stable sensor response.

Specific Aim #3: Development of FRET nanoprobes based on gold nanoparticles as quenchers interfaced to organic fluorophores and immobilized onto optical fibers. It is hypothesized that gold nanoprobes would provide an enhanced response and better sensitivity.

Specific Aim #4: Design a protocol for the future development of other specific mycoplasma sensors utilizing the FRET technique. Eventually, we want to develop this type of sensor so it can be used to accurately and quickly detect various high consequence pathogens of interest in national bio-defense efforts.

CHAPTER 3

IN SOLUTION FRET SENSOR DEVELOPMENT

3.1 INTRODUCTION

The goal of this series of experiments was to develop and test a FRET nanoprobe pair to detect *M. capricolum* in solution. Our hypothesis is that the antibody will undergo a conformational change when exposed to the peptide or the organism. This conformational change would be detected by the organic fluorescent nanoprobes that were used to label the key components of the detection system.

This goal was accomplished by examining three different antibodies specific for the mycoplasma bacteria. Each antibody will be labeled with a donor fluorophore and incubated with different concentrations of a protein labeled with another fluorophore. This protein will bind preferentially to the Fc region of the antibody (Protein G) or to the Fab region of the antibody through interaction with the light chain (Protein L). The location of the protein binding helps ensure that the FRET phenomenon will occur between the two fluorophores. The fluorescence will be measured by using a bench-top spectrofluorometer. The resulting fluorescence will then be examined to determine the optimal A/D ratio, which is the ratio of acceptor fluorophore to donor fluorophore for optimal detection. Once the optimal A/D ratio is determined for each bioprobe (detection recognition elements in this case, the Protein-Fluorophore—Antibody-Fluorophore complex), they will then be exposed to a specific antigen and/or a non specific antigen to

determine if there is a conformational change corresponding to the specific antigen. These changes will be measured by use of a ratiometric method described below.

The antibody-protein complex that demonstrates the largest conformational change at the optimal A/D ratio will be exposed to varying amounts of the specific antigen (both peptide and mycoplasma) to determine if there is a defined dose response. The dose response experiments will be performed with both Protein G and Protein L, in order to determine the effects of the different binding locations on the response of the sensor. Lastly, a detection complex involving Protein L conjugated to the donor fluorophore and Protein G conjugated to the acceptor fluorophore, and both proteins bound to the antibody at their preferential binding locations will be used to examine the sensor response.

3.2 MATERIALS

3.2.1 FRET ANTIBODIES AND ANTIGENS

The current study employs the following materials related to the VmcE and VmcF lipoproteins of *M. capricolum*; these were provided by Kim Wise, Department of Molecular Microbiology and Immunology at the University of Missouri-Columbia:

1. Synthetic peptides representing the repeat structures of VmcF (pep F) or VmcE (pep E): These soluble peptides are essentially monovalent in terms of the epitopes recognized by the MAbs (monoclonal antibodies).

2. Murine MAbs raised to conjugated pep E (α-pep E) or pep F (α-pep F_1; and α-pep F_2): These MAbs had been purified by affinity chromatography using protein G; they were of the IgG 1 or IgG2b subclass and contained kappa light chains.

3. Paraformaldehyde-fixed cells of cultured *M capricolum*: These fixed organisms are highly polyvalent, although the exact dimensions of spacing of the proteins on the surface is not known.

Prior to the studies outlined in this thesis, the MAbs, peptides and fixed organisms had been shown specifically to bind and/or inhibit as cognate partners in ELISA and Western blot assays, and were highly selective in this regard.

3.2.2 FRET PROTEINS

Protein A and Protein G which bind the Fc region of the antibody, and Protein L which binds the Fab' region of the antibody were all purchased from Sigma in St. Louis, MO. These proteins provided some control over the placement of the donor and acceptor fluorophores on the antibody.

3.3 METHODS

3.3.1 CONJUGATION OF PROTEINS TO FRET DYES (ACCEPTOR)

Proteins A, Protein G, Protein L were all labeled under non-denaturing conditions with Alexa Fluor 594, the acceptor fluorophore, according to the procedure modified from Molecular Probes (Eugene, OR). The proteins conjugated to the fluorophores were allowed to dialyze for 4 days in order to remove the unbound fluorophores instead of running the protein conjugated dyes through a size exclusion column.

3.3.2 CONJUGATION OF ANTIBODIES TO FRET DYES (DONOR)

All IgG antibodies were labeled with the Alexa Fluor 546, the donor fluorophore, according to the procedure from Molecular Probes.

3.3.3 MOLARITY AND F/P RATIO CALCULATION

The molarity of the protein conjugated to the fluorophore is calculated by the equation:

$$[M] = \frac{(A_{280}-(A_{max}* 0.12))*DF}{203000}$$

Equation 3.1- Molarity Equation

The correction factor for the fluorophore's contribution to the absorbance at 280 nm is 0.12 for AF546 and 0.56 for AF594. DF is the dilution factor of the solution. 203000 is the molar extinction coefficient (ε) in $cm^{-1}M^{-1}$ of a typical IgG at 280 nm.

The F/P Ratio is a measure of the degree of labeling. The ratio is determined by the moles of fluorophore to the moles of protein. This ratio is calculated for each protein-fluorophore conjugation using the equation:

$$F/P = \frac{A_{max} * DF}{\varepsilon_{dye} * [M]}$$

Equation 3.2- Fluorophore per Protein Ratio

where A_{max} is the absorbance at the maximum excitation wavelength of the fluorophore used in the conjugation (558 nm for AF546 and 590 nm for AF594), DF is the dilution factor, ε_{dye} is the molar extinction coefficient at the maximum wavelength (ε_{AF546}= 104000 $cm^{-1}M^{-1}$ and ε_{AF594}=73000 $cm^{-1}M^{-1}$), and [M] is the molarity of the protein. This ratio is then used to determine the optimal acceptor fluorophore to donor fluorophore ratio for the antibody-donor fluorophore—protein-acceptor fluorophore complex.

3.3.4 OPTIMAL A/D RATIO DETERMINATION

Acceptor to donor ratio (A/D) is the number of acceptor fluorophores to the number of donor fluorophores on a protein-antibody complex. This is determined from the calculated F/P ratios of the antibody and the protein, as well as the molarity for the fluorophore conjugated to the antibody and for the fluorophore conjugated to the protein. The number of moles for the donor and the acceptor are calculated by taking the amount added to the solution divided by the molecular weight (150,000g/mol for the antibodies and 45,000g/mol for the protein). Then the number of moles of fluorophore is calculated

by using the F/P ratio. Then the A/D ratio is calculated by taking the number of moles of the acceptor fluorophore and dividing it by the number of moles of the donor fluorophore. The optimal A/D ratio is determined by examination of donor and acceptor emission peaks at various concentrations. Various ratios were prepared by keeping the amount of antibody-donor constant and varying the amount of protein-acceptor. These can be seen in Table 3.1.

Table 3.1-Experiment Setup for Optimal A/D Determination Experiments

α-pep E			
A/D Ratio	Sample	Amt. Donor (μg) (AF546-a-pep E)	Amt. Acceptor (μg) (AF594-PG)
	1	0	0.25
0.76	2	1.25	0.5
0.89	3	1.25	0.25
0.36	4	1.25	0.1
α-pep F_1			
A/D Ratio	Sample	Amt. Donor (μg) (AF546-a-pep F1)	Amt. Acceptor (μg) (AF594-PG)
	1	0	0.25
0.83	2	1	0.5
0.42	3	1	0.25
0.17	4	1	0.1
α-pep F_2			
A/D Ratio	Sample	Amt. Donor (μg) (AF546-a-pep F2)	Amt. Acceptor (μg) (AF594-PA)
	1	0	0.25
1.75	2	1	0.5
0.88	3	1	0.25
0.35	4	1	0.1

The solutions were incubated overnight at 4 degrees C and then scanned using the spectrofluorometer, ISA Fluoromax-3. Having an optimal A/D ratio is critical for the most efficient energy transfer between the donor and acceptor fluorophores. Too much of either fluorophore can lead to self-quenching while too little can produce non-detectable signals caused by insufficient energy transfer.

3.3.5 IN SOLUTION DETECTION OF ANTIGEN

Each of the α-pep Antibody-AF546 and PG-594 were incubated over night at 4 degrees C based on their optimal A/D Ratios. Each individual antibody-AF546—PG-AF594 solution was then distributed into three separate micro-cuvettes; a control, a specific antigen test (for the α-pep E, 1.33µl of peptide E was added and for α-pep F_1 and α-pep F_2, 1.33 µl of pep F was added), and a non-specific antigen test (for the for the α-pep E, 1.33µl of peptide F was added and for α-pep F_1 and α-pep F_2, 1.33 µl of pep E was added). Then PBS was added to each micro-cuvette in order to bring the final volume up to 100 µl. The solutions were agitated gently to ensure mixing and then allowed to incubate for 1 hour at room temperature. Before scanning with the spectrofluorometer, the final volume of each micro-cuvette was increased with PBS to aid in measuring with the spectrofluorometer. The wavelength for excitation of the donor fluorophore was 555nm to initiate FRET between the AF546 and the AF594 and the change in the fluorescence between the donor and acceptor fluorophores was recorded between 565nm and 650nm.

Table 3.2 – Molarities during the In-Solution Testing

Antibody	Components	Molarity		Amounts	
		incubation (in 100 μl)	scanning (in 500 μl)	incubation (in 100 ul)	scanning (in 500 μl)
α-pep E	Donor	83.3 nM	8.33 nM	12.5 ng/μl	2.5 ng/μl
	Acceptor	6.67 nM	0.67 nM	1 ng/μl	0.2 ng/μl
	Peptide	13.3 μM	2.66 μM	1.33 μl of 1 mM stock	Diluted into 500 μl
α-pep F1					
	Donor	66.7 nM	6.67 nM	10 ng/μl	1ng/μl
	Acceptor	6.67 nM	0.67 nM	1 ng/μl	0.1 ng/μl
	Peptide	13.3 μM	1.33 μM	1.33 μl of 1 mM stock	Diluted into 1000 μl
α-pep F2					
	Donor	66.7 nM	6.67 nM	10 ng/μl	1 ng/μl
	Acceptor	6.67 nM	0.67 nM	1 ng/μl	0.1 ng/μl
	Peptide	13.3 μM	1.33 μM	1.33 μl of 1 mM stock	Diluted into 1000 μl

The results are then calculated by using a ratiometric method:

Without Antigen (Control):

$$R1 = \frac{\bar{I}(Donor\lambda\ Range)}{\bar{I}(Acceptor\lambda\ Range)}$$

Equation 3.3- Control Ratio

With Addition of Specific or Non-Specific Antigen:

$$R2 = \frac{\bar{I}(Donor\ \lambda\ Range)}{\bar{I}(Acceptor\ \lambda\ Range)}$$

Equation 3.4- Specific or Non-Specific Ratio

Ratio of Ratio Measurement:

$$R3 = \frac{R2}{R1}$$

Equation 3.5- Ratio of Ratio Measurement

I is the average intensity of fluorescence. The donor range is 565nm to 575 nm. The acceptor range is 605 to 615 nm. There will be a R3 value for both the specific and non-specific antigen.

3.3.6 IN-SOLUTION DOSE RESPONSES

Each of the α-pep Antibody-AF546 and PG-594 were incubated over night at 4 degrees C based on their optimal A/D Ratios. Nine different samples were prepared at the same A/D ratio (A/D = 1.32). Each sample contained 1 μg of donor and 0.6 μg of acceptor. The specific peptide antigen was added at various concentrations (26.6pg/ml, 13.3pg/ml, 6.65pg/ml, 3.33pg/ml, 1.66pg/ml, 0.8pg/ml, 0.4pg/ml, 0.2pg/ml, and 0.1pg/ml). Then PBS was added to each micro-cuvette in order to bring the final volume up to 100 μl. The solutions were agitated gently to ensure mixing and then allowed to incubate for 1 hour at room temperature. Before scanning with the spectrofluorometer, the final volume of each micro-cuvette was increased to 500μl with a 400μl addition of PBS. The wavelength for excitation of the donor fluorophore was set to 555nm to initiate FRET between the AF546 and the AF594 and the change in the fluorescence between the donor and acceptor fluorophores was recorded between 565nm and 650nm. This was also

repeated for the fixed *M. capricolum* at various concentrations (45ng/ml, 22.5ng/ml, 11.25ng/ml, 5.63ng/ml, 2.81ng/ml, 1.41ng/ml, 0.7ng/ml, 0.35ng/ml, and 0.18ng/ml). The ratiometric analysis mentioned above was used to analyze the data.

3.4 RESULTS AND DISCUSSION

3.4.1 α-PEP E A/D DETERMINATION AND ANTIGEN SPECIFICITY

Results--

Results for the optimal A/D ratio for the α-pep E is showed in Figure 3.1. The fluorescent scans in Figure 3.1 contained equal amounts of donor and decreasing amounts of acceptor. The solution with an A/D ratio of 1.76 contained 1.25μg of donor and 0.5μg of acceptor. The A/D ratio of 0.89 only had 0.25μg of acceptor while the A/D ratio of 0.36 had 0.1μg of acceptor. All of the solutions were graphed versus a sample containing only 0.25μg of acceptor to serve as a control to compare the A/D ratios. Also noticeable is a slight baseline shift that can be seen in A/D ratio 1.76.

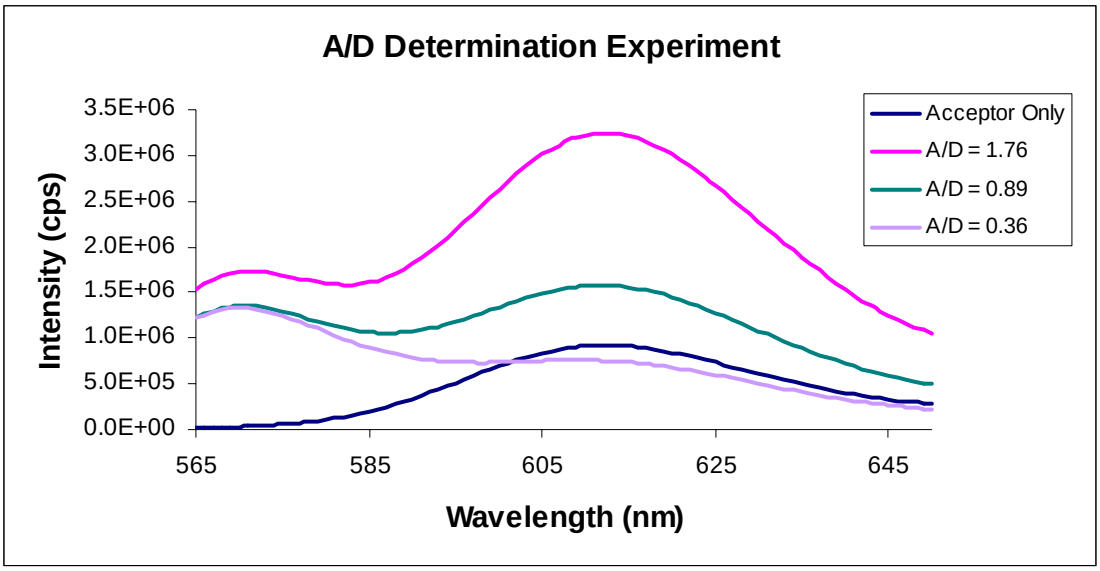

Figure 3.1—A/D Determination Experiment for α-pep E

In Figure 3.2, the results for the antigen specificity for α-pep E at A/D = 0.36 are shown. For each sample 1.33μl of peptide antigen was added to compare responses. This test was performed 4 times. The average R3 values for the specific and non-specific are respectively 1.018 and 0.994. Figure 3.2 shows that the non-specific response is larger than compared to the specific response. Performing the paired T-Test on the two series of data gives us a p-value of 0.205. Setting the $\alpha = 0.2$, this p-value indicates that this data may or may not be statistically significant (the p-value should be less than α). This means that this test is inconclusive to determine if there was a significant difference between the specific and non-specific response.

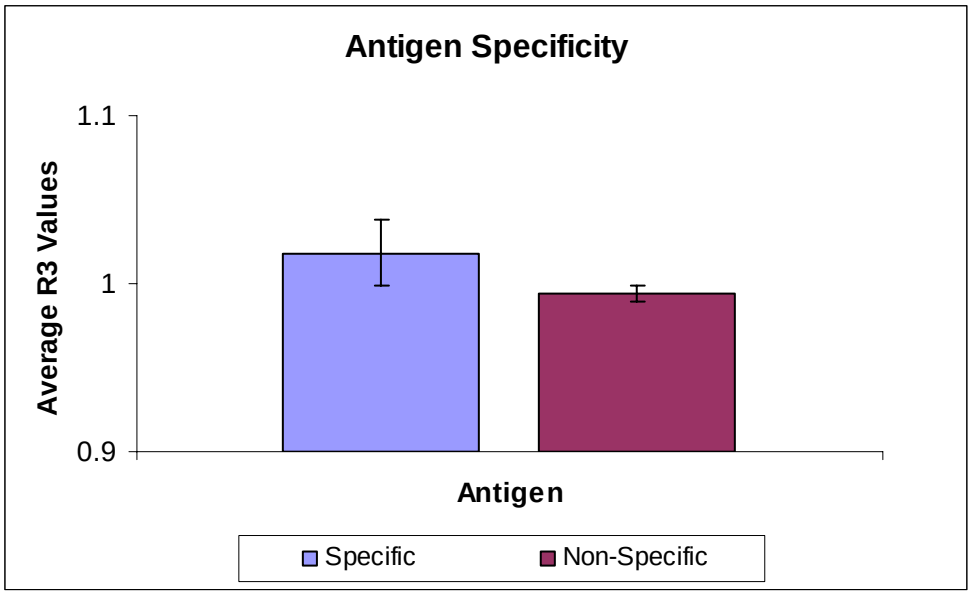

Figure 3.2—The Antigen Specificity Experiment for α-pep E at A/D = 0.36

Discussion—

Figure 3.1 shows that as the A/D ratio increased, the acceptor peak increased in intensity. For an optimal A/D ratio, too much of either fluorophore can lead to non-detectable signals due to self quenching while too little of either fluorophore will result in non-detectable signals due to too little energy transfer. In this case, the optimal A/D ratio was selected to be 0.36. It had a donor peak that had a higher intensity compared to the acceptor peak which indicates that enough donor fluorophore is present to transfer energy to the acceptor fluorophore. There was also enough acceptor fluorophore to measure any increase in intensity.

Figure 3.2 shows that there is 2.4% difference between the specific and non-specific response and the standard deviations were calculated to be 0.04 and 0.01 respectively.

The average R3 values for the specific and non-specific were respectively 1.018 and 0.994. A response of approximately 1 for the non-specific was expected, since the non-specific antigen should not bind or elicit any changes in antibody conformation. However, when an antibody binds to a specific antigen, the antibody may have three different reactions. One reaction involves the antibody undergoing a conformational change, forcing the Fab arm regions to separate, i.e., the hinge angle to increase. In this scenario, the FRET that occurs would result in a decrease in the donor fluorescence and an increase in acceptor fluorescence, thus a decrease in the R3 value. A second scenario involves that antibody undergoing a conformational change, forcing the Fab arm regions closer to together, i.e., decreasing the hinge angle. Thus, an increase in the R3 value as the donor increases and the acceptor decreases. A final reaction is that the antibody does not undergo a conformational change. In this case, the FRET technique would not be a viable solution to detect *M. capricolum*.

The results of this first experiment are inconclusive. It appeared that the antibody may have undergone a conformational change, but the results are not significant. The possibility also exists that a larger A/D ratio would have given better results. .For example, an A/D ratio between 0.36 and 0.86 may have provided better energy transfer due to the increased number of acceptor fluorophores.

3.4.2 α-PEP F_1 A/D DETERMINATION AND ANTIGEN SPECIFICITY

Results--

Like the solutions in Figure 3.1, the A/D ratio solutions in Figure 3.3 contained equal amounts of donor and decreasing amounts of acceptor. The solutions imparting a ratio of 0.83 contained 1.00μg of donor and 0.5μg of acceptor. The A/D ratio of 0.42 only had 0.25μg of acceptor while the A/D ratio of 0.17 had 0.1μg of acceptor. The fluorescence spectra of these solutions were graphed versus a solution containing only 0.25μg of acceptor to serve as a control to compare the A/D ratios. A slight baseline shift can be seen among the donor peaks.

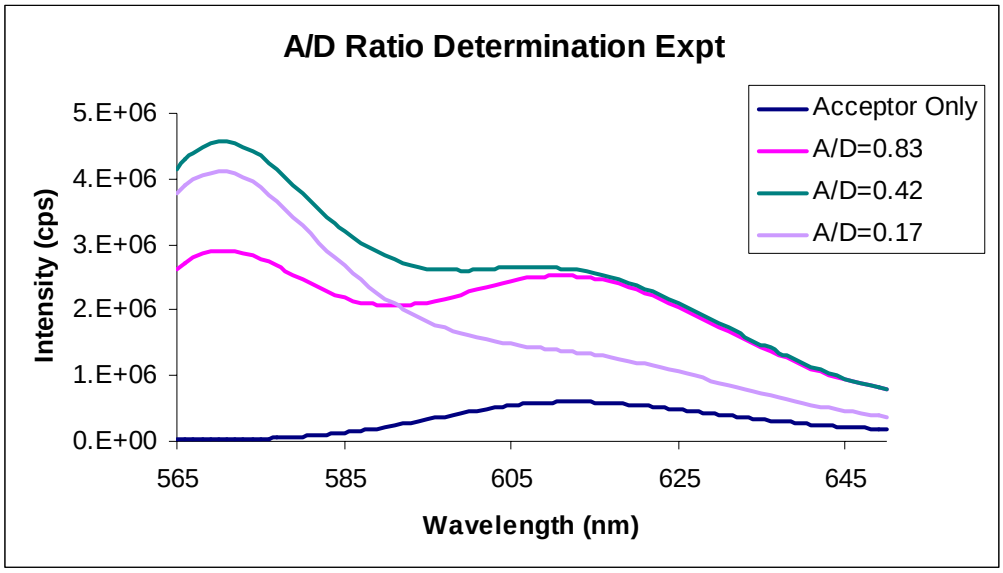

Figure 3.3—A/D Determination Experiment for α-pep F_1

Figure 3.4 shows the results of the antigen specificity tests. The A/D ratio of 0.17 was utilized for these tests. For each solution, 1.33µl of peptide antigen was added to determine if the antibodies would undergo a conformational change. This test was performed 4 times. The average R3 values for the specific and non-specific are respectively 1.007 and 0.953. Figure 3.4 shows that the non-specific response is larger as compared to the specific response. Performing the paired T-Test on the two series of data gives a p-value of 0.211. Setting the $\alpha = 0.2$, this p-value indicates that this data was not quite statistically significant (the p-value should be less than α). This means that there is not a significant difference between the specific and non-specific response.

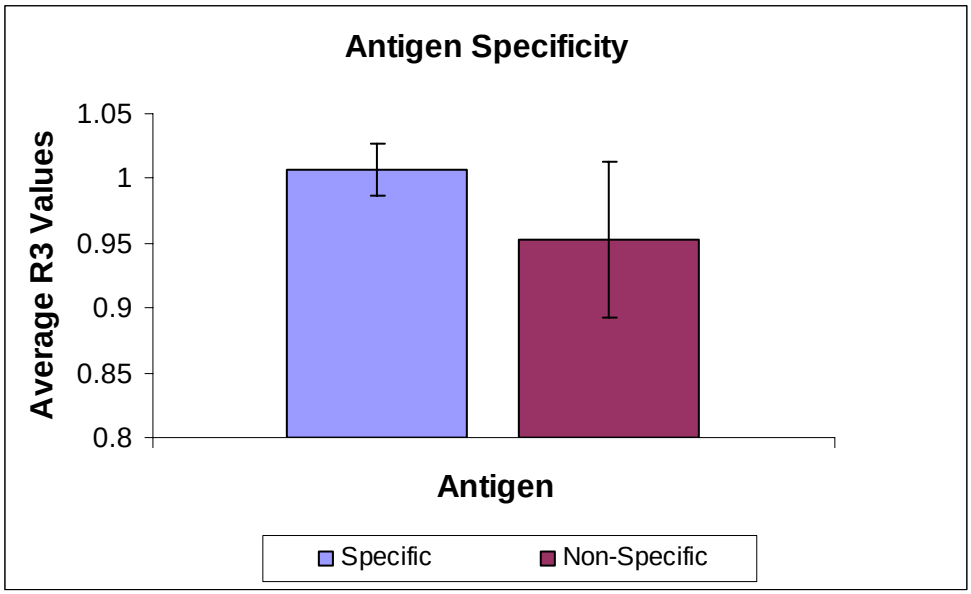

Figure 3.4—The Antigen Specificity Experiment for α-pep F_1 at A/D = 0.17

Discussion—

Figure 3.3 shows that as the A/D ratio increased, the acceptor peak increased in intensity. As mentioned above, for an optimal A/D ratio, too much of either fluorophore can lead to non-detectable signals due to self quenching while too little of either fluorophore will result in non-detectable signals due to too little energy transfer. In this case, the optimal A/D ratio was selected to be 0.17. It had a donor peak that had a higher intensity compared to the acceptor peak which indicates that enough donor fluorophore is present to transfer energy to the acceptor fluorophore. There was also enough acceptor fluorophore to measure any increase in intensity. However, a better selection for the A/D ratio would have been 0.42. This value still displayed a high donor peak while also displaying a measurable acceptor peak. The A/D ratio of 0.17 may not have had enough acceptor fluorophores.

The average R3 values for the specific and non-specific are respectively 1.007 and 0.953. The specific response of approximately 1 indicates that there was no conformational change over the background noise. Figure 3.4 shows that there is 5.5% difference between the specific and non-specific responses. The standard deviations were calculated to be 0.05 and 0.11 respectively. The standard deviation of the specific response was very small, which indicates that this response is relatively stable. The standard deviation of the non-specific response, however, was quite large compared to the specific response which means that its response was not quite as stable.

These results could indicate several different things. One possibility is that there was no measurable conformational change when the specific antigen bound the antibody, due to poor A/D ratio selection. Another possibility is that there was no conformational change with this particular antibody. A third option is that the antigen binding to the antibody caused a decrease in the angle of the hinge region of the antibody instead of the expected increase. The possibility also exists that a larger A/D ratio would have had better results.

3.4.3 α-PEP F_2 A/D DETERMINATION AND ANTIGEN SPECIFICITY

Results—

The A/D ratio samples in Figure 3.5 contained equal amounts of donor and decreasing amounts of acceptor. The sample giving a ratio of 1.75 contained 1.00 μg of donor and 0.5μg of acceptor. The A/D ratio of 0.88 only had 0.25μg of acceptor while the A/D ratio of 0.35 had 0.1μg of acceptor. All of these were graphed versus a sample containing only 0.25μg of acceptor to serve as a control to compare the A/D ratios. A distinct baseline shift can be seen. Since the entire donor amounts were the same, they should be at approximately the same location on the graph.

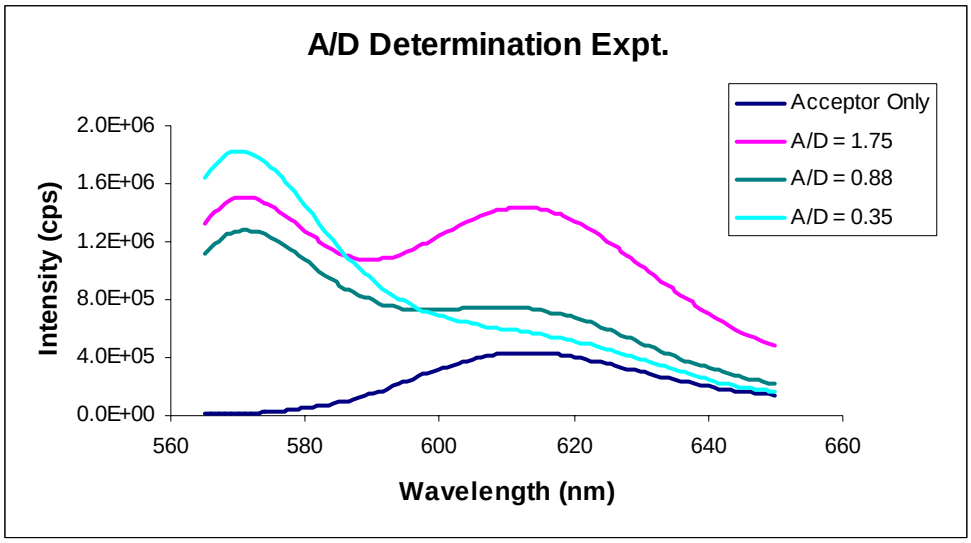

Figure 3.5—A/D Determination Experiment for α-pep F_2

Figure 3.6 displays the results from the antigen specificity tests. A solution with an A/D ratio of 0.35 was utilized. For each solution, 1.33µl of peptide antigen (specific and non-specific) was added to determine if a conformational change in the antibody occurs. This test was performed 5 times. The average R3 values for the specific and non-specific are respectively 0.997 and 0.970. Figure 3.6 shows that the non-specific response is larger as compared to the specific response. Performing the paired T-Test on the two series of data gives us a p-value of 0.6458. Setting the $\alpha = 0.2$, this p-value indicates that this data is definitely not close enough to be statistically significant (the p-value should be less than α). This means that there is a not significant difference between the specific and non-specific response.

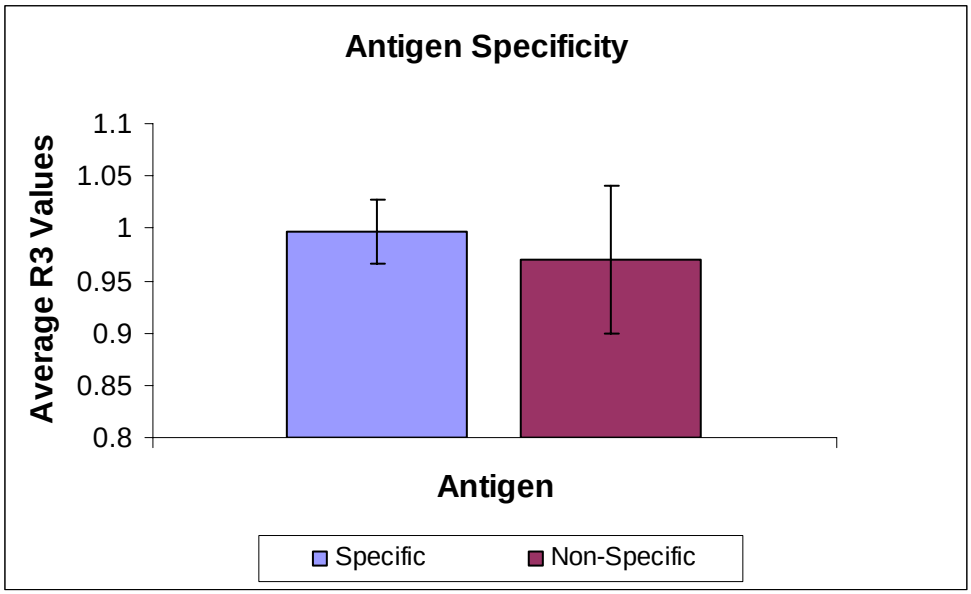

Figure 3.6—The Antigen Specificity Experiment for α-pep F_2 at A/D = 0.35

Discussion—

Figure 3.5 shows that as the A/D ratio increased, the acceptor peak increased in intensity. Too much of either fluorophore can lead to non-detectable signals due to self quenching while too little of either fluorophore will result in non-detectable signals due to too little energy transfer. In this case, the optimal A/D ratio was selected to be 0.35. It had a donor peak that had a higher intensity compared to the acceptor peak which indicates that enough donor fluorophore is present to transfer energy to the acceptor fluorophore. There was also enough acceptor fluorophore to measure any increase in intensity. However, again it is noted that the optimal A/D ratio was most likely not chosen. The A/D ratio of 0.88 would have provided more acceptor molecules to be utilized in the FRET reaction.

In Figure 3.6 the average R3 values for the specific and non-specific are respectively 0.997 and 0.970. The specific response of approximately 1 indicates that there was no conformational change over the background noise. Figure 3.6 shows that there is 2.7% difference between the specific and non-specific responses. The standard deviations were calculated to be 0.05 and 0.14 respectively. The standard deviation of the specific response was very small, which indicates that this response is relatively stable. The standard deviation of the non-specific response, however, was quite large compared to the specific response which means that its response was not nearly as stable. Again, these results could indicate the same possibilities that have been previously described.

Of the three different antibodies, a-pep F1 gave the largest change in responses as well as a small p-value. This antibody was selected to be further examined in the dose response tests.

3.4.4 DOSE RESPONSES

The next set of experiments investigated the response of the antibody-PG complex to different dosages of antigens. In other words, we wanted to see if a bigger response in R3 values would occur if more antigens were added.

Results—

The response of the bioprobes to the mycoplasma organisms is displayed in Figure 3.7 and 3.8. Each of the dose response experiments was run 5 different times. A very slight increasing trend in the R3 values can be seen from the largest concentration of antigen

(45ng/ml) to the smallest concentration of antigen (0.18ng/ml). For example, there is a 16% change in response with addition of 45ng/ml of antigen. However, there is a similar response (a 15% change) with the addition of 2.81ng/ml. The smallest response (a 8% change) occurred with the addition of 0.7ng/ml instead of with the expected addition of the smallest amount of antigen (0.18ng/ml). This general increasing trend in R3 values demonstrates a decreasing response as the concentration decreases. No distinct increase in response (decrease in R3 value) can be seen at incremental additions of antigen. The calculated standard deviations ranged from small (0.01) to large (0.06).

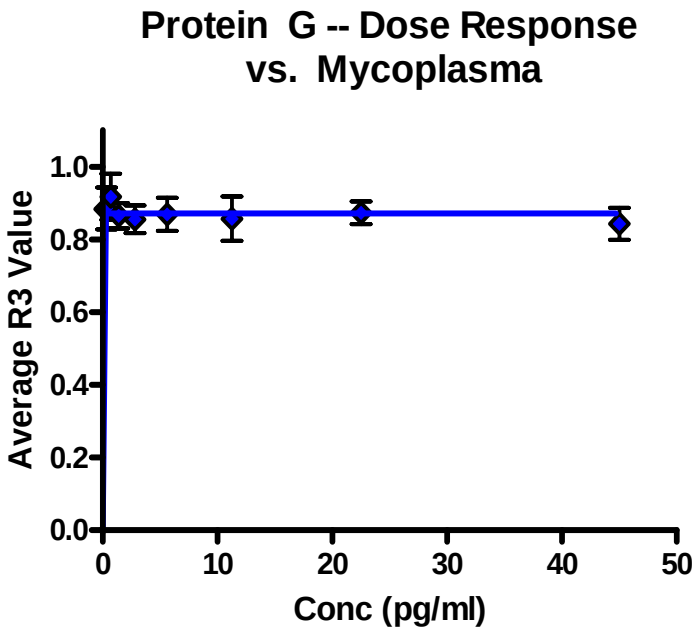

Figure 3.7 –-Dose Responses for the Protein G Acceptor against the Mycoplasma Bacteria

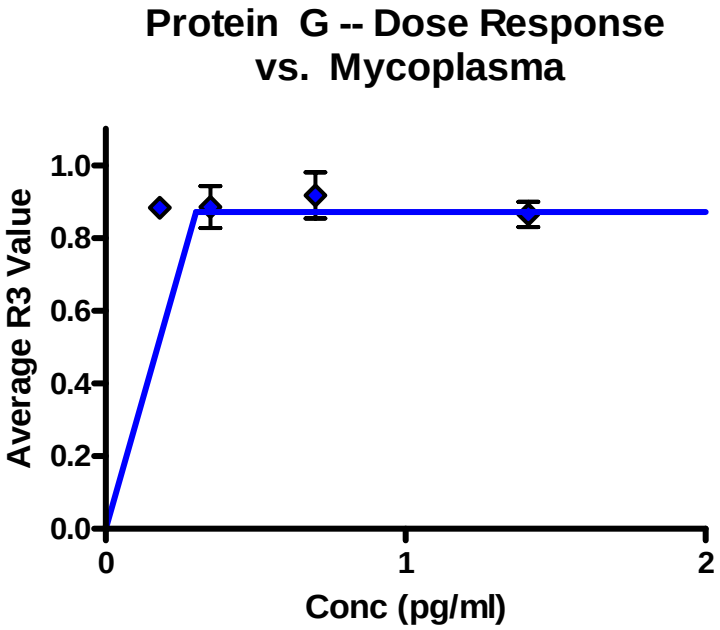

Figure 3.8 –Low-level Dose Responses for the Protein G Acceptor against the Mycoplasma Bacteria

Each of the dose response experiments was run 5 different times. These results are displayed in Figure 3.9 and Figure 3.10. They show the response of the bioprobes when exposed to different concentrations of the peptide. These dose response experiments were run 5 different times. As shown in Figure 3.8 a very small response (a 5% change in the R3 values) can be seen with the smallest addition of antigen (0.18ng/ml). Figure 3.8 also displays some very good responses (large changes in the R3 values) with a couple of the larger additions of antigen. For example, with the addition of 11.25ng/ml there was the best response with an 18% change. Another good response (a 17% change) can be seen with the addition of 22.5ng/ml. However, there were some poor responses in the mid-range of the concentrations added. This can be seen when 2.81ng/ml was added

to the sample. This produced only a 8% change in the R3 value. The next smaller addition (1.41ng/ml) produced a much larger change in the R3 value (a 14% change). The calculated standard deviations varied from 0.02 to 0.1.

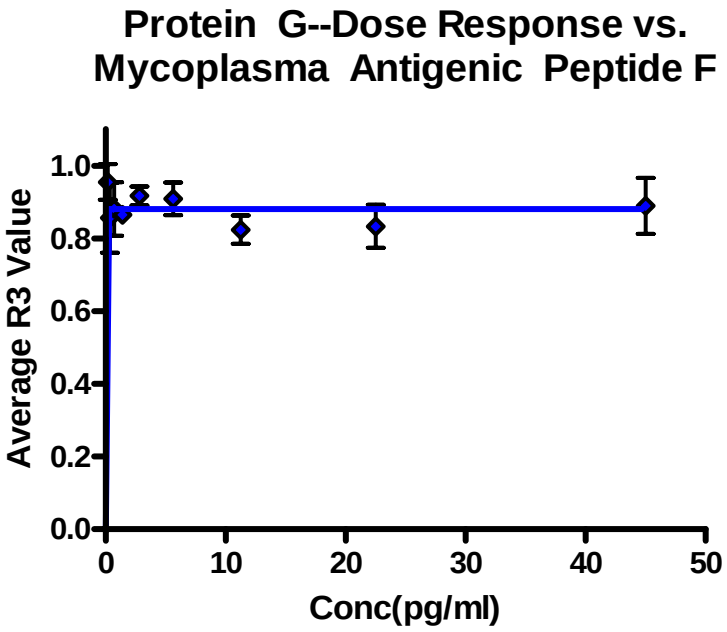

Figure 3.9 –-Dose Responses for the Protein G Acceptor against the Mycoplasma Antigenic Peptide F

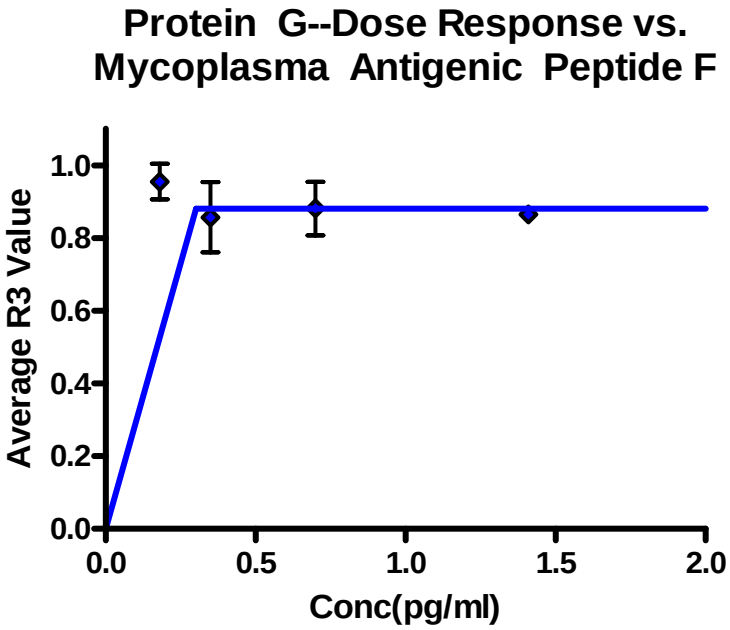

Figure 3.10 —Low-level Dose Responses for the Protein G Acceptor against the Mycoplasma Antigenic Peptide F

Discussion—

Figures 3.7 and 3.9 (and therefore 3.8 and 3.10) indicate that when the antigen binds the antibody, there is an increase in the angle of the hinge (the two Fab regions of the antibody become further apart or "opens"). Figure 3.7 (the PG-Mycoplasma experiment) shows the least variation in standard deviation of the three types of experiments performed, ranging from 0.01 to 0.06. This indicates that the bioprobe setup has the least variable response of the three. This is promising, since these accomplish one of the specific aims.

The above experiments were examined to determine if a calibration equation could be seen. Theoretically, if there is a predictable dose response, there should either be a distinct increase (a decrease in the angle of the hinge region or "closes") or decrease (an increase in the angle of the hinge region or "opens") in the R3 value with the addition of increasing amounts of antigen. In this case, we would expect low R3 values with the addition of larger amounts of antigen and higher R3 values with smaller additions of antigen. This, however, is not the case in this circumstance. The above experiments show that this particular biosensor is not able to track the dose response of a particular sample. This means that there is not a fixed response for a specific amount of antigen added. Therefore, this sensor is not able to be calibrated to detect different amounts of antigen. This was expected for the in-solution experiments because the probes have a tendency to interact with each other as they are free-floating in solution. For example, an acceptor on one antibody could be receiving energy from a donor on an antibody in close proximity. This situation is not necessarily a problem since it is desirable to be able to detect trace amounts of mycoplasmas as an earlier warning system. However, when the bioprobes are immobilized on an optical fiber, we expect a more predictable response. The optical fiber should give an increased response due to the increased sensitivity of the fiber's light gathering ability.

Predicting the dose response for mycoplasmas is not critical. In the event of a mycoplasma infection, earlier detection is key. For this sensor, we want the lowest limit of detection possible. In Figure 3.7, the smallest amount of antigen added resulted in an average of a 12% change in R3 value. This sensor can successfully detect 0.18ng/ml

with a good response. This response suggests that the biosensor system can be used to detect even trace amounts.

The above experiments also indicate that use of the mycoplasma as the antigen produced a more stable biosensor response than the mycoplasma antigenic peptide. Lastly, it was shown that this biosensor detection system is able to detect 0.18ng/ml with a 12% change in response with the ability to possibly detect smaller concentrations.

3.4.5 PROTEIN L-PROTEIN G TRIAL

Results—

A new bioprobe was constructed and tested. The donor fluorophore was conjugated to the Protein L and the acceptor fluorophore was conjugated to the Protein G. This particular method imparts more control over the placement of the fluorophores which leads to less background noise. These two proteins were added in alternating order (but at the A/D ratio of 2.21) to determine which provided a better complex in which to detect the antigen. In (Ab-PG-PL) the antibody, the Protein G, and the Protein L were added at the same time. In (Ab+PG)-PL the antibody and Protein G were allowed to incubate for an hour, and then the Protein L was added and allowed to incubate with the (Ab+PG) complex for an hour. In (Ab+PL)-PG the antibody and Protein L were allowed to incubate for an hour, and then the Protein G was added and allowed to incubate with the (Ab+PL) complex for an hour. These three were run against the Antibody only (Ab), the Protein L only (PL), and the Protein G only (PG). The spectra can be seen in Figure 3.10.

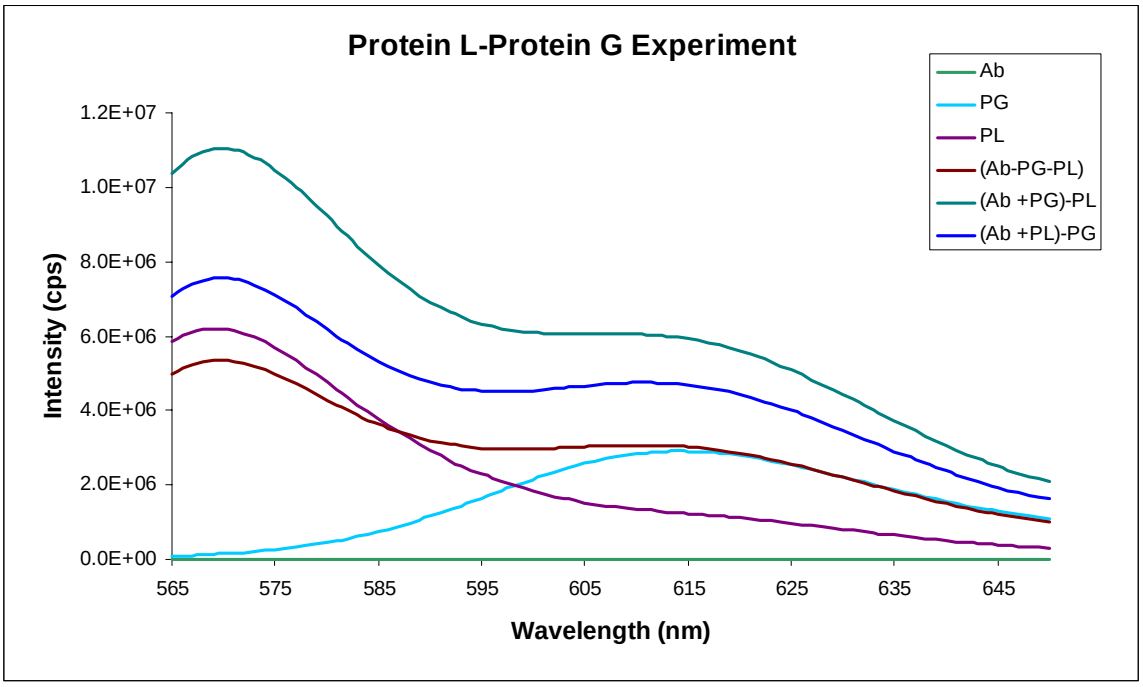

Figure 3.10 –-Protein G and Protein L Test for FRET

The (Ab+PL)-PG complex shows the most acceptor fluorescence. This is approximately measured from the valley between the donor and acceptor peak (about 598nm) and the peak of the acceptor peak (about 610nm). The (Ab+PL)-PG complex acceptor peak gives a 242058cps (counts per second) rise in intensity. The next highest was the (Ab-PG-PL) complex giving an intensity rise of 103084cps. Finally, the (Ab+PG)-PL complex gave the lowest intensity increase at 1160cps.

Next, the bioprobes were exposed to the specific antigens. The experiment summarized in Figure 3.11 was run twice with additions of 1.33µl of peptide antigen. The (Ab-PG-PL) complex showed the best response of the three as compared with the control (a 7%

change in R3 value). The other two complexes (the (Ab+PG)-PL and the (AB+PL)-PG) showed very little response, their average values were very close to the control (where R3 = 1). However, their standard deviations were quite small (0.01 and 0.02, respectively) as compared to the standard deviation of the (Ab-PG-PL) complex (0.06). The p values in relation to the control were 0.62 for the (Ab-PG-PL) complex, 0.58 for the (Ab+PG)-PL complex, and 0.55 for the (Ab+PL)-PG complex. The high p-values indicate that the results of these experiments are not statistically significant (when the α value is set at 0.2).

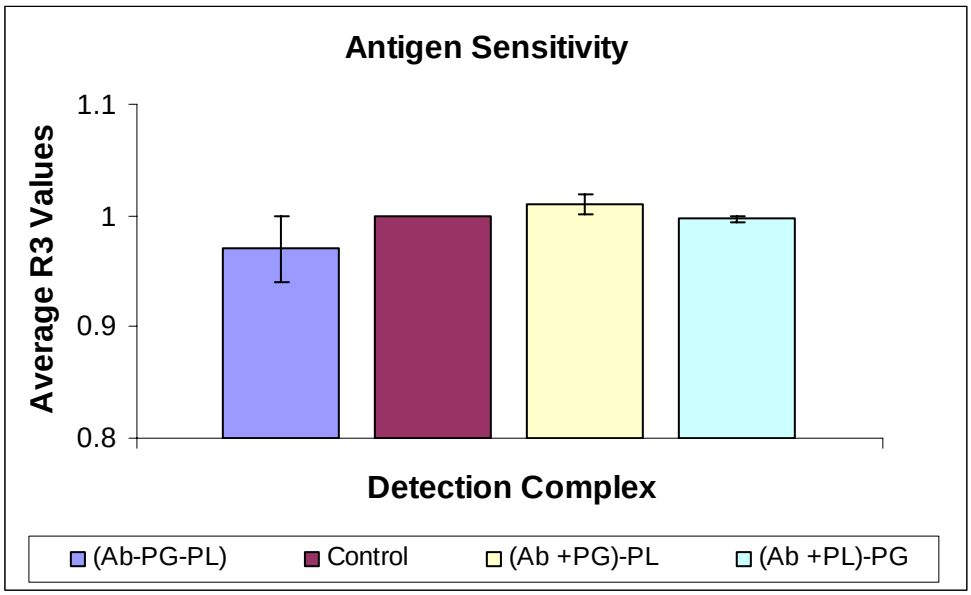

Figure 3.11—The Antigen Specificity Experiment for Protein G and Protein L

Discussion--

Figure 3.10 shows that each of the three complexes displays some acceptor fluorescence when excited at 555nm. However, the (Ab+PL)-PG complex provided the most acceptor

fluorescence of the three, so this particular construction most likely favored or promoted more PG binding.

The antigen specificity experiment showed that the (Ab-PG-PL) complex had the best response of the three different complexes. However, it had the largest standard deviation by far (0.06 as compared to 0.02 and 0.01). This signifies that the (Ab-PG-PL) response is not as stable as the (Ab+PG)-PL response or the (AB-PL)-PG response. Protein L was tried in this sensor setup due to its unique ability to selectively bind the Fab region of the antibody. But, this type of configuration does not seem to indicate that it is conducive to steady-state sensing. So, even though we expected better stability using Protein L, Protein L may be hindering binding of the antigen to the antibody. Thus, it was decided to continue with Protein G.

3.5 CONCLUSION

The α-pep F_1 gave the largest change in responses as well as a small p-value. This antibody was selected to be examined further in the immobilization onto an optical fiber and in the gold nanoparticle system. The above experiments also indicated that the use of the mycoplasma as the antigen produced a more stable biosensor response than the mycoplasma antigenic peptide. These experiments also concluded that in-solution dose responses are not conducive to calibrated responses. The response will be examined in an optical fiber system to determine if a distinct dose response can be achieved. Lastly, it was shown that the Protein G-pep F bioprobes were able to detect very small concentrations of mycoplasmas.

CHAPTER 4

FIBER OPTIC FRET SENSOR IMMOBILIZATION

4.1 INTRODUCTION

The goal of specific aim #2 was to examine the immobilization of the FRET nanoprobes to optical fibers and to test the biosensor response. It was hypothesized that immobilization of the nanoprobes would result in a stable sensor response. These tests were performed by immobilizing the detection complex onto an optical fiber via silanization. These optical fibers were exposed to varied concentrations of both the mycoplasma bacteria and the mycoplasma surface peptide antigen and then dose response were recorded using a Fluoromax-3 bench-top spectrofluorometer with fiber optic attachment.

4.2 MATERIALS

4.2.1 FRET ANTIBODIES AND ANTIGENS

The current study employs the following materials related to the VmcE and VmcF lipoproteins of *M. capricolum*; these were provided by Kim Wise, Department of Molecular Microbiology and Immunology at the University of Missouri-Columbia:

1. Synthetic peptides representing the repeat structures of VmcF (pep F) or VmcE (pep E): These soluble peptides are essentially monovalent in terms of the epitopes recognized by the MAbs (monoclonal antibodies).

2. Murine MAbs raised to conjugated pep E (α-pep E) or pep F (α-pep F_1; and α-pep F_2): These MAbs had been purified by affinity chromatography using protein G; they were of the IgG 1 or IgG2b subclass and contained kappa light chains.

3. Paraformaldehyde-fixed cells of cultured *M capricolum*: These fixed organisms are highly polyvalent, although the exact dimensions of spacing of the proteins on the surface is not known.

Prior to the studies outlined in this thesis, the MAbs, peptides and fixed organisms had been shown specifically to bind and/or inhibit as cognate partners in ELISA and Western blot assays, and were highly selective in this regard.

4.2.2 FRET PROTEINS

Protein G binds the Fc region of the antibody, and was purchased from Sigma in St. Louis, MO. PG was labeled with an acceptor dye, Alexa-Fluor 594, via a modified labeling kit from Molecular Probes (now called Invitrogen). Additionally, the antibodies were labeled with Alexa-Fluor 546 using a similar labeling kit. The proteins conjugated to the dyes were allowed to dialyze for 4 days to remove the unbound dye instead of running the protein conjugated dyes through a size exclusion column.

4.2.3 SILANIZATION CHEMICALS

MTS ((3-Mercaptopropyl)trimethoxysilane FLUKA, Cat. No. 63800) and DMF (N-formyldimethylamine, FLUKA Cat. No.40240) were obtained from Sigma-Aldrich (St. Louis, MO). GMBS (N-Succinimidyl 4-maleimidobutyrate, Pierce Prod. No. 22309) a heterobifunctional cross-linker that is reactive towards amino and sulfhydryl groups, was obtained from Pierce Biotechnology (Rockford, IL).

4.3 METHODS

4.3.1 CONJUGATION OF PROTEINS TO FRET DYES (ACCEPTOR)

Protein G was labeled with Alexa Fluor 594 to act as an acceptor dye according to the procedure from Molecular Probes. This protein will bind the Fc portion of the antibody.

4.3.2 CONJUGATION OF ANTIBODY TO FRET DYES (DONOR)

All IgG antibodies were labeled with the Alexa Fluor 546 to act as a donor dye according to the procedure from Molecular Probes.

4.3.4 ETCHING OF OPTICAL FIBERS

Silica optical fibers were purchased from Thor Labs (Newton, NJ). The fibers were multi-mode, step index fibers with a 400 μm silica core and a very thin polymer cladding. The distal ends of the optical fibers were immersed in hydrofluoric acid for 2-4 hours to allow etching by capillary action forming a taper in order to enhance signal acquisition.

The tips of the fibers were then rinsed in distilled water and examined under a microscope to ensure the tips had a smooth taper. The cladding of the fiber tips was removed approximately a half centimeter past the taper.

4.3.5 CLEANING OF OPTICAL FIBER

The fiber tips were then cleaned and silanized using a procedure published by Bhatia (Bahatia, 1989). The tips of the optical fibers were immersed in a 50:50 volume mix of 100% hydrochloric acid and 100% methanol for 30 minutes then rinsed in double distilled water. The tips were then immersed in 100% concentrated sulfuric acid for 30 minutes and then rinsed twice in double distilled water to remove any residues. Finally, the fiber tips were placed in a beaker of boiling double distilled water for 30 minutes and allowed to air dry.

4.3.6 SILANIZATION OF PG OPTICAL FIBER

The clean, dry fiber tips were positioned in a glove bag under a nitrogen atmosphere. They were then immersed in a 2% v/v of MTS ((3-Mercaptopropyl)trimethoxysilane FLUKA, ca no. 63800) in toluene for two hours then rinsed in toluene for 3 minutes and allowed to air dry. The fiber tips were next immersed into a 2mM solution of GMBS (N-Succinimidyl 4-maleimidobutyrate, FLUKA. Cat no. 63175) in absolute ethanol for 1 hour. The GMBS was prepared by dissolving approximately 50 μl of DMF (N-formyldimethylamine) for 4ml volume of ethanol. The tips were then rinsed in PBS for 3 minutes. The fiber tips were then incubated overnight at 4 degrees Celsius with a 50

μl/ml solution of Alexa Fluor 594 conjugated Protein G in PBS. They were then rinsed in PBS three times for 5 minutes and then scanned to provide a background.

4.3.7 BINDING OF ANTIBODY TO IMMOBILIZED PG

After immobilization of the PG-acceptor to the fibers, the fibers were then immersed in a 50 μl/ml solution of Alexa Fluor 546 conjugated IgG in PBS and allowed to incubate overnight at 4 degrees Celsius. They were then rinsed in PBS for 5 minutes and then scanned to provide the background FRET control reading.

4.3.8 DOSE RESPONSES ON AN OPTICAL FIBER

The fiber optic biosensors were exposed to high (3ng/ml), medium (5.63pg/ml), and low (0.18pg/nl) concentrations of peptide antigen or the fixed *M. capricolum* and the resulting fluorescence were recorded on the spectrofluorometer with the fiber optic attachment. The overall setup can be seen in Figure 4.1, while a close up of the stage can be seen in Figures 4.2 and 4.3. Three different filters are utilized on this stage a 530DF30 excitation filter (yellow label in Figure 4.2 and 4.3), a 550DCSP dichromatic short pass filter (blue label), and a HQ560LP (green label) a low pass emission filter. First, the excitation light passes through the excitation filter (specific for a 540nm excitation wavelength). Then the enduring light will pass through the dichromatic short pass filter (present so that the wavelengths lower than 550 can be passed while the higher wavelengths are filtered). Finally, the remaining light will pass through the emission long pass filter (passes the light that has wavelengths higher than 560). The resulting light is able to reach the detector.

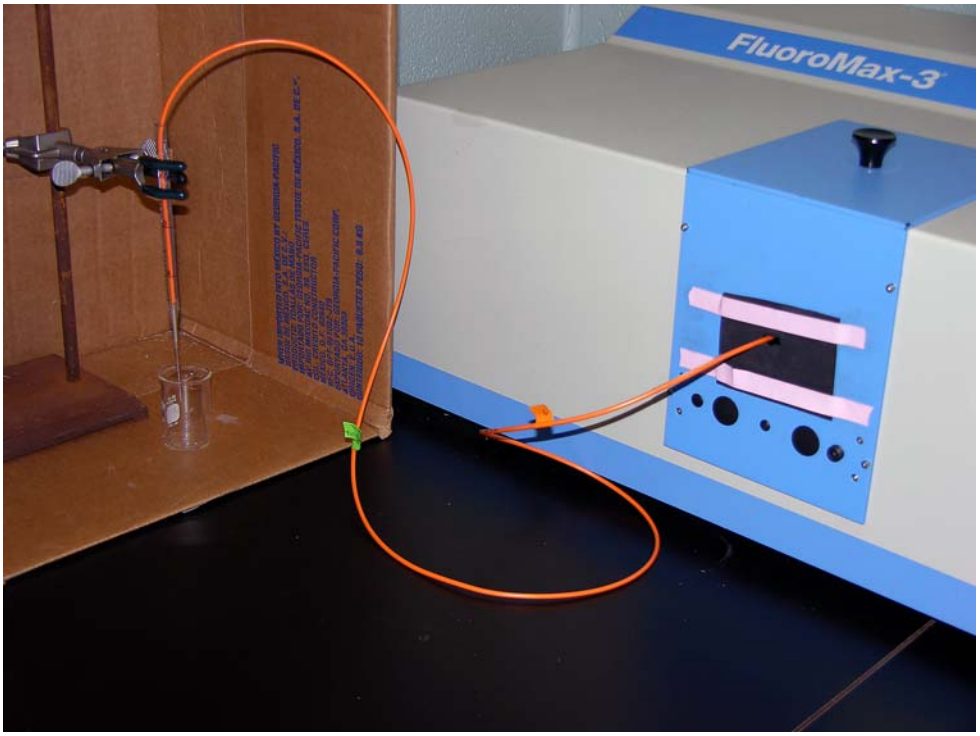

Figure 4.1—Basic setup for testing the optical fibers

Figure 4.2—First close up of fiber optic stage within the bench-top spectrofluorometer

Figure 4.3—Second close up of the fiber optic stage

4.3.9 MEASUREMENT OF FRET ACTIVITY

The results were then calculated by using a ratiometric method:

Before Addition of Antigen (Control):

$$R1 = ControlPeakRange$$

Equation 4.1—Average Control Value

After Addition of Specific Antigen:

$$R2 = TestPeakRange$$

Equation 4.2—Average Specific Value

Ratio of Measurements:

$$R3 = \frac{R2}{R1}$$

Equation 4.3—Ratio of Measurements

I is the average intensity of fluorescence. The "Control Peak Range" is the average of intensity values from 565nm to 575nm before the addition of antigen and "Test Peak Range" is the average of intensity values from 565nm to 575 nm after the addition of antigen.

4.3 RESULTS AND DISCUSSION

4.3.1 IMMOBILIZATION OF DETECTION COMPLEX

Results—

Figure 4.1 shows two fluorescent spectra of the PG-antibody complex immobilized to an optical fiber. The blue line is the spectrum with immobilized Protein G on the surface. The Protein G was conjugated to the acceptor fluorophore. When excited with a 555nm wavelength of light, the acceptor emits at a wavelength of approximately 615nm. The pink line is the spectrum from the same optical fiber with the Protein G silanized to the surface and then incubated with a 50μg/ml solution of the antibody (AB) conjugated to the donor dye. When the donor dye is excited with 555nm wavelength of light, it emits at approximately 570nm.

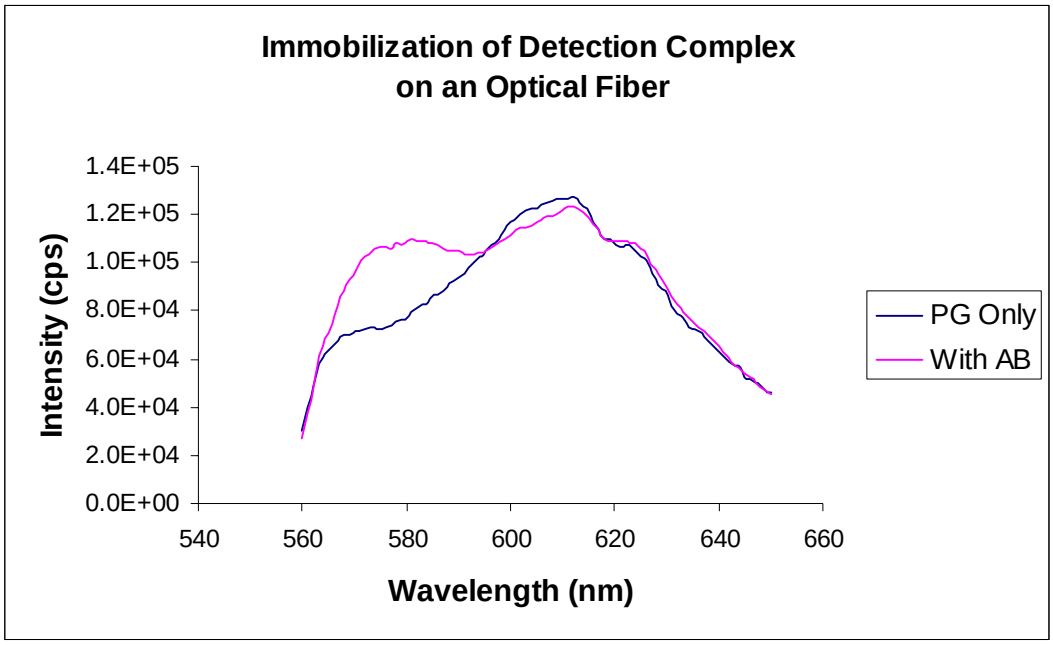

Figure 4.4—Immobilization on an Optical Fiber

Discussion--

Protein G is immobilized onto the fibers as noted by the acceptor peak in Figure 4.4. The purpose of this particular experiment was to determine if Protein G would still bind to the antibody (Ab) after being silanized to the surface of the optical fiber. Figure 4.1 shows that Protein G remains functional after immobilization. This was demonstrated this by the appearance of the donor peak, caused by the binding of the antibody to the immobilized Protein G. These results lead to the conclusion that the detection complex (the AF594-Protein G—AF546-α-pep F_1 complex) was successfully immobilized to the optical fiber.

4.3.2 *M. CAPRICOLUM* DOSE RESPONSE

Results—

Figure 4.5 displays the dose response of the biosensor against the mycoplasma organism. The series of experiments was run five times at three different concentrations: high (3ng/ml), medium (5.63 pg/ml), and low (0.18pg/ml). At the high concentration the average response was 0.97 with a standard deviation of 0.07. The middle concentration had an average response of 1.02 with a standard deviation of 0.05. The average response of the low concentration was 0.91 with a standard deviation of 0.14. In other words, the best response (a 9% change) occurred with the smallest concentration of mycoplasma bacteria. The t-test was performed on the five values of each concentration versus the control (where the R3 value equals 1). The three p-values were 0.521 (high), 0.496 (medium), and 0.245 (low). The p-value for the low concentration is close to the chosen α for this experiment ($\alpha = 0.20$) which means that the response is inconclusive in whether there is statistical significance.

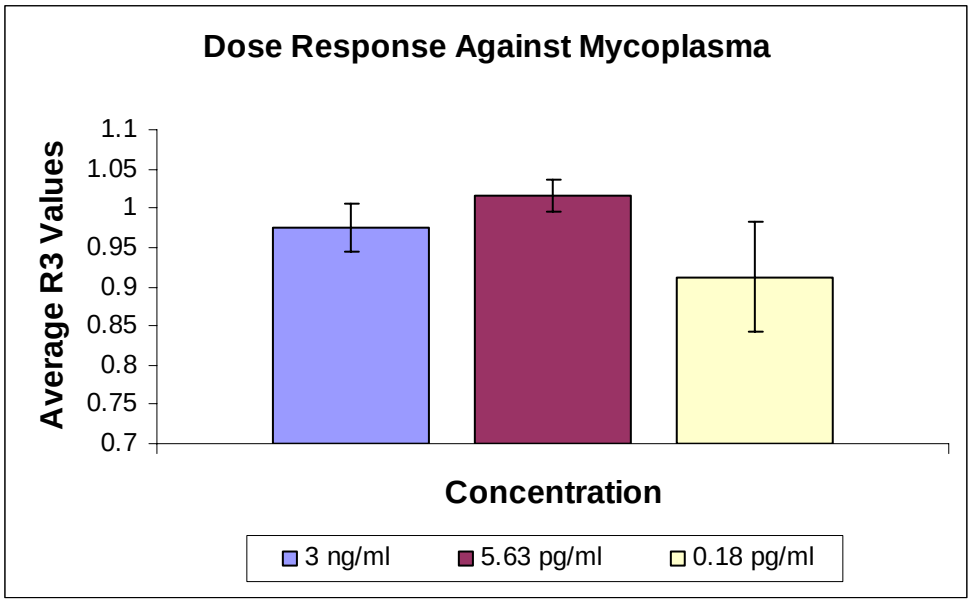

Figure 4.5—*M. capricolum* Dose Response Experiment

Discussion—

All the trials in Figure 4.5 (and below in Figure 4.6) were exposed to the same concentrations of Protein G and α-pep F_1 during the silanization/immobilization process. This means that the packing densities of the detection complexes on the surface of the optical fiber are all approximately the same. It was expected that the higher concentration of mycoplasma would give a more significant (and thus stronger) response. Therefore, it was surprising that the low concentration of mycoplasma gave a more significant response than those of the higher concentrations. This indicates that the low concentration of mycoplasma allows easier access to the immobilized detection complexes and thus elicits a more efficient energy transfer. In the case of the higher concentrations it is possible that the higher concentrations of mycoplasmas disrupted the binding mechanisms of the detection complex, which would cause poor energy transfer

from the donor to the acceptor. In other words, the binding capacity of the biosensor was saturated. It is encouraging that this biosensor can detect very low concentrations of the mycoplasmas even though it does not have the ability to provide quantitative data. The largest benefit of this sensor setup is that it does provide a very low limit of detection for early warning systems.

4.3.3 *M. CAPRICOLUM* ANTIGENIC PEPTIDE DOSE RESPONSE

Results—

Figure 4.6 displays the results of the dose response of the fiber optic biosensors against the antigenic peptides. The experiment was performed three times with the same concentrations used above. In this case, the average response of the 3ng/ml addition was 1.09 with a standard deviation of 0.22. The average response of the 5.63 pg/ml addition was 0.957 with a standard deviation of 0.063. Lastly, the 0.18pg/ml addition gave a response of 0.981 with a standard deviation of 0.231. So, of the three, the addition of 5.63pg/ml gave the best response (a change of 4.3%), with the 3ng/ml addition giving the worst response.

The t-test was performed and gave p-values of 0.566 (high), 0.357 (medium), and 0.903 (low). This indicates that of the responses were not statistically significant. In other words, the p-values were all greater than the α chosen for these experiments (α=0.20).

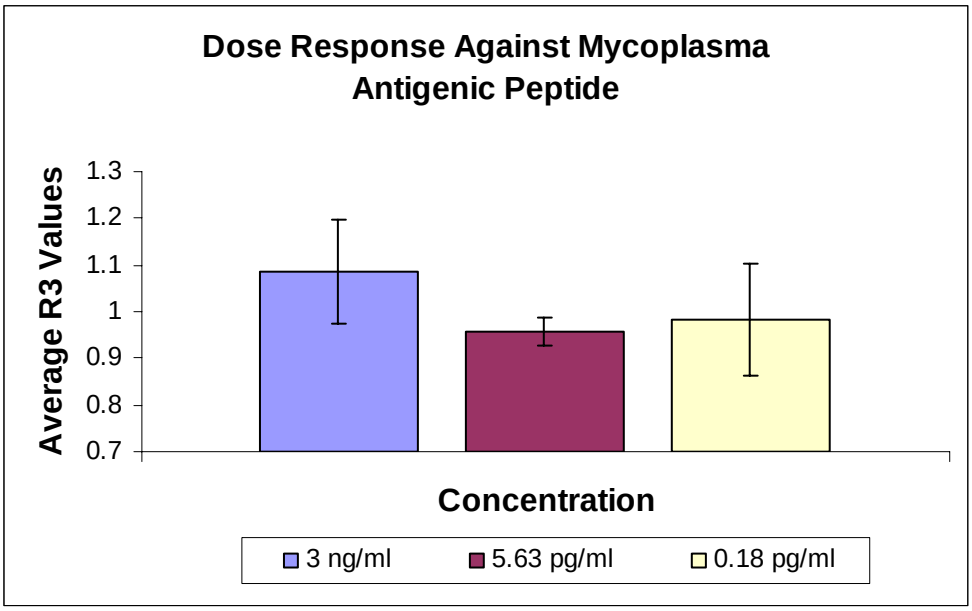

Figure 4.6—*M. capricolum* Antigenic Peptide Dose Response Experiment

Discussion--

At the lowest concentration (0.18pg/ml), the biosensor did not give a significant response. Figure 4.6 demonstrates that the lowest dose was too low for a detectable change in signals. The 5.63pg/ml addition provided a good change in fluorescence, but the response was not significant. One would expect that the highest concentration would elicit the most significant response. Surprisingly, this did not occur. Again, this may be due to saturation of the detection complex as explained above. It is also possible that the antigenic peptides do not elicit a conformational change in the antibodies.

4.4 CONCLUSION

The detection complexes appeared to undergo conformational changes when silanized to the surface of the optical fiber and then exposed to the mycoplasma organisms. Thus, the experiments in this chapter demonstrated that the requirements for Objective # 2 were met. In other words, the objective of developing a fiber optic biosensor to detect mycoplasmas was successful. However, there were some surprises. The mycoplasma exhibited a lower detection limit than the peptides and the data for the mycoplasma were more significant. This is probably due to the fact that the mycoplasmas have a stronger influence on conformational change than the peptides. The higher concentrations appeared to saturate the immobilized detection complexes and prevented a conformational change. In conclusion, this fiber optic biosensor appears to be able to detect mycoplasmas at very low concentration levels. However, these particular sensors are unable to give significant quantitative data. More test need to be performed to optimize the A/D ratios and the packing density of the complexes onto the optical fibers. This sensor appears to be best suited as an early warning system to quickly and accurately detect the presence of *M. capricolum*.

CHAPTER 5

FIBER OPTIC FRET SENSOR IMMOBILIZATION WITH GOLD NANOPARTICLES

5.1 INTRODUCTION

Specific aim #3 is addressed in this chapter. The goal of this series of experiments is to develop a FRET nanoprobe sensor based on gold nanoparticles as quenchers interfaced to organic fluorophores and immobilized onto optical fibers. Our hypothesis is that gold nanoprobes will provide an enhanced response and better sensitivity than the sensor based on two organic fluorophores. The set of experiments were performed using the same protocol detailed in Chapter 4. The detection complex will be immobilized onto an optical fiber by silanization. These optical fibers will be exposed to varied concentrations of mycoplasma bacteria and then the dose response will be recorded via a Fluoromax-3 bench-top spectrofluorometer with fiber optic adaptor.

5.2 MATERIALS

5.2.1 FRET ANTIBODIES AND ANTIGENS

The current study employs the following materials related to the VmcE and VmcF lipoproteins of *M. capricolum*; these were provided by Kim Wise, Department of Molecular Microbiology and Immunology at the University of Missouri-Columbia:

1. Synthetic peptides representing the repeat structures of VmcF (pep F) or VmcE (pep E): These soluble peptides are essentially monovalent in terms of the epitopes recognized by the MAbs (monoclonal antibodies).

2. Murine MAbs raised to conjugated pep E (α-pep E) or pep F (α-pep F_1; and α-pep F_2): These MAbs had been purified by affinity chromatography using protein G; they were of the IgG 1 or IgG2b subclass and contained kappa light chains.

3. Paraformaldehyde-fixed cells of cultured *M capricolum*: These fixed organisms are highly polyvalent, although the exact dimensions of spacing of the proteins on the surface is not known.

Prior to the studies outlined in this thesis, the MAbs, peptides and fixed organisms had been shown specifically to bind and/or inhibit as cognate partners in ELISA and Western blot assays, and were highly selective in this regard.

5.2.2 FRET PROTEINS (QUENCHER)

Protein G binds the Fc region of the antibody. This particular Protein G-gold nanoparticle complex (PG-G) was purchased from Sigma in St. Louis, MO.

5.2.3 SILANIZATION CHEMICALS

MTS ((3-Mercaptopropyl)trimethoxysilane FLUKA, Cat. No. 63800) and DMF (N-formyldimethylamine, FLUKA Cat. No.40240) were obtained from Sigma-Aldrich (St.

Louis, MO). GMBS (N-Succinimidyl 4-maleimidobutyrate, Pierce Prod. No. 22309) a heterobifunctional cross-linker that is reactive towards amino and sulfhydryl groups, was obtained from Pierce Biotechnology (Rockford, IL).

5.3 METHODS

5.3.1 CONJUGATION OF ANTIBODY TO FRET DYES (DONOR)

All IgG antibodies were labeled with the Alexa Fluor 546 (AF546) to act as a donor dye according to the procedure from Molecular Probes.

5.3.3 ETCHING OF OPTICAL FIBERS

The distal end of the 400 nm optical fibers were immersed in hydrofluoric acid for 2-4 hours to allow etching by capillary action forming a taper in order to enhance signal acquisition. The tips of the fibers were then rinsed in distilled water and examined under a microscope to ensure the tips had a smooth taper. The cladding of the fiber tips was removed approximately a half centimeter past the taper.

5.3.4 CLEANING OF OPTICAL FIBER

The fiber tips were then cleaned and silanized using a procedure published by Bhatia. The tips of the optical fibers were immersed in a 50:50 volume mix of 100% hydrochloric acid and 100% methanol for 30 minutes then rinsed in double distilled water. The tips were then immersed in 100% concentrated sulfuric acid for 30 minutes

and then rinsed twice in double distilled water to remove any residues. Finally, the fiber tips were placed in a beaker of boiling double distilled water for 30 minutes and allowed to air dry.

5.3.5 SILANIZATION OF PG-G TO OPTICAL FIBER

The clean, dry fiber tips were positioned in a glove bag under a nitrogen atmosphere. They were then immersed in a 2% v/v of MTS in toluene for two hours then rinsed in toluene for 3 minutes and allowed to air dry. The fiber tips were next immersed into a 2mM solution of GMBS in absolute ethanol for 1 hour. The GMBS was prepared by dissolving approximately 50 μl of DMF for 4ml volume of ethanol. The tips were then rinsed in PBS for 3 minutes. The fiber tips were then incubated overnight at 4 degrees Celsius with a 50 μl/ml solution of Protein G-gold nanoparticle complexes in PBS. Finally, the fiber tips were then rinsed in PBS three times for 5 minutes and then scanned with the Fluoromax-3 spectrofluorometer to provide a background.

5.3.6 ANTIBODY BINDING TO IMMOBILIZED PG-G

After rinsing the fibers in PBS for 3 minutes, the fibers were then immersed in a 50 μl/ml solution of Alexa Fluor 546 conjugated IgG in PBS. These were then allowed to incubate overnight at 4 degrees Celsius. The fibers were then scanned with the Fluoromax-3 spectrofluorometer to provide the background FRET control reading.

5.3.7 DOSE RESPONSES ON AN OPTICAL FIBER

The fibers were then exposed to high (3.0 ng/μl), medium (5.63 pg/μl), and low (0.18 pg/μl) concentrations of peptide antigen or the fixed M. cap and the responses were recorded on the Fluoromax-3 spectrofluorometer. The same optical fiber setup that was used for Chapter 4 was used again in this chapter.

5.3.8 MEASUREMENT OF FRET ACTIVITY

The results were then calculated by using a ratiometric method:

Before Addition of Antigen (Control):

$$R1 = ControlPeakRange$$

Equation 5.1—Average Control Value

After Addition of Specific Antigen:

$$R2 = TestPeakRange$$

Equation 5.2—Average Specific Value

Ratio of Measurement:

$$R3 = \frac{R2}{R1}$$

Equation 5.3—Ratio of Measurement

I is the average intensity of fluorescence. The “Control Peak Range” is the average of intensity values from 565nm to 575nm before the addition of antigen and “Test Peak Range” is the average of intensity values from 565nm to 575 nm after the addition of antigen.

5.3 RESULTS AND DISCUSION

5.3.1 QUENCHING OPTICAL FIBER SYSTEM

Results—

Figure 5.1 shows three different fluorescent spectra. The blue line is the spectrum with the Protein G-gold nanoparticle complex immobilized on the surface of a silica optical fiber. The pink line is the spectrum from the same optical fiber with the Protein G-gold nanoparticle complex silanized to the surface and then incubated with a 50μg/ml solution of the antibody (AB) conjugated to the donor dye. When the donor dye is excited with 555nm wavelength of light, it emits at approximately 570nm. The green line is the spectrum after the addition of the antigen.

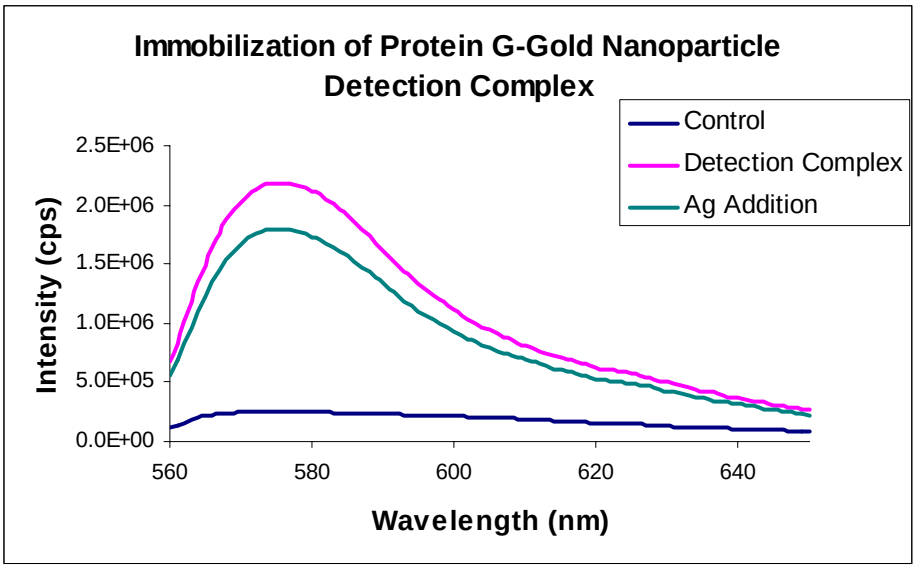

Figure 5.1- Immobilization of Protein G-Gold Nanoparticles on an Optical Fiber

Discussion--

Figure 5.1 shows that there is a decrease in intensity of the donor peak with addition of the various concentrations of mycoplasma. The purpose of this particular experiment was to determine if the Protein G-gold nanoparticle complex would still bind to the antibody (Ab) after being silanized to the surface of the optical fiber. Figure 5.1 shows that Protein G-gold nanoparticle complex remains functional after immobilization. This was demonstrated this by the appearance of the donor peak, caused by the binding of the antibody to the immobilized Protein G-gold nanoparticle complex. These results lead to the conclusion that the detection complex (the Protein G-gold nanoparticle—AF546-α-pep F_1 complex) was successfully immobilized to the optical fiber.

5.3.2 *M. CAPRICOLUM* DOSE RESPONSE

Results—

Figure 5.2 and 5.3 displays the dose response of the biosensors when exposed to mycoplasmas. The experiment was run five times. Each of these experiments included tests at three different concentrations: 3.00ng/ml (high), 5.63pg/ml (medium), and 0.18pg/ml (low). The average response for the 3.00ng/ml addition was 1.04 with a standard deviation of 0.12. The next lowest response was 0.18 pg/ml, with an average response of 1.02 and a standard deviation of 0.06. The lowest response was from the 5.63pg/ml addition of mycoplasma bacteria. The average response was 0.99 with a standard deviation of 0.02. This particular response gave the most stable response of the three. The paired t-test was used to analyze the statistical significance of the response. The p-values were 0.462 (high), 0.599 (medium), and 0.514 (low). All of these values were well above the $\alpha = 0.20$ chosen, which indicates that these responses are not really statistically significant.

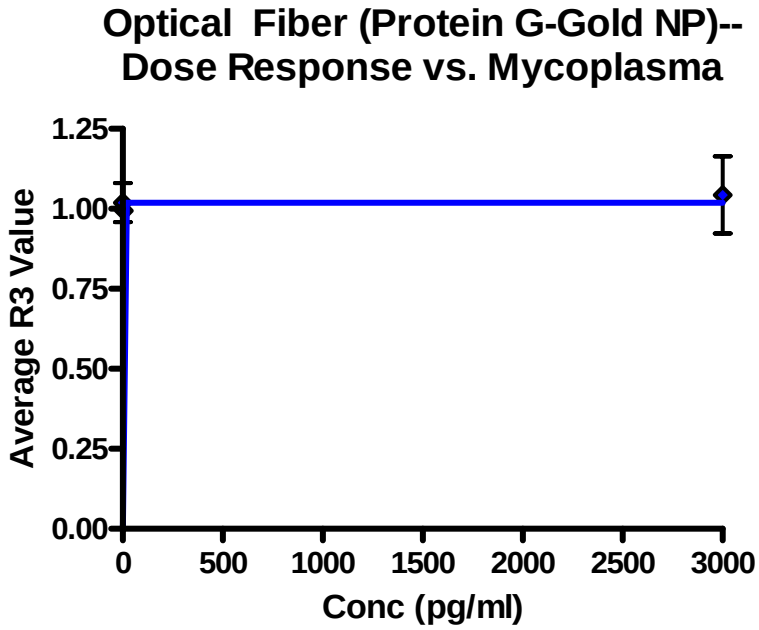

Figure 5.2- Dose Response Experiment against *M. capricolum*

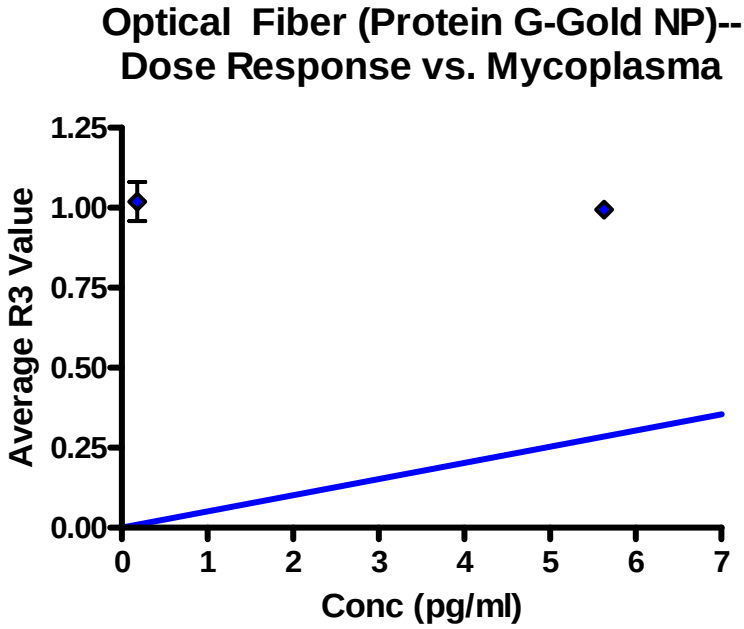

Figure 5.3- Low-level Dose Response Experiment against *M. capricolum*

This experiment was run five different times. Each of these experiments (seen in Figures 5.2 and 5.3 above) included tests at three different concentrations: 3.00ng/ml (high), 5.63pg/ml (medium), and 0.18pg/ml (low). The average response for the 3.00ng/ml addition was 1.04 with a standard deviation of 0.12. The next lowest response was 0.18pg/ml, with an average response of 1.02 and a standard deviation of 0.06. The lowest response was from the 5.63pg/ml addition of mycoplasma bacteria. The average response was 0.99 with a standard deviation of 0.02. This particular response gave the most stable response of the three. The paired t-test was used to analyze the statistical significance of the response. The p-values were 0.462 (high), 0.599 (medium), and 0.514 (low). All of these values were well above the $\alpha = 0.20$ chosen, which indicates that these responses are not really statistically significant.

Discussion--

Analysis of Figure 5.2 and 5.3 did not indicate any significant changes in conformation with addition of various concentrations of mycoplasmas. Several factors are capable of effecting these measurements. Since we are just measuring the quenching of the donor fluorescence, background shifts could possibly occur before and after the scans. The first scan was taken prior to mycoplasma exposure while the second scan was taken one hour after exposure. Another factor includes lengthy incubation time after addition of the mycoplasmas. The mycoplasmas could bind the antibodies and then release. This shouldn't occur due to the binding affinity between the antibody and the specific antigen, the binding is strong, but not as strong as a covalent bond. Another factor that could

effect the measurement would be shifting of the filters within the bench-top spectrofluorometer. Other factors include variances in the packing density and in the number of gold nanoparticles. Too few gold nanoparticles would not give the desired quenching effect.

5.4 CONCLUSION

Gold nanoparticles are well known quenchers. This sensing technique should have provided good data on the conformational changes. Since it failed to do so, it was concluded that the parameters of this technique were not optimized. Further testing would need to be performed in order to conclude if this is a viable method for *M. capricolum* detection. In other words, Objective #3 needs further experimentation in the examination of the quenching parameters.

CHAPTER 6

CONCLUSIONS

The overall objective of this research was to develop a novel FRET immunosensor to detect the caprine pathogen *M. capricolum*. The research had four main goals:

1) to develop and test FRET nanoprobes to detect *M. capricolum* in solution,
2) to immobilize the FRET nanoprobes to optical fibers to test the biosensor response,
3) to develop FRET nanoprobes based on gold nanoparticles as quenchers interfaced to organic fluorophores and immobilize this detection complex onto optical fibers,
4) to design a protocol for the future development of other specific mycoplasma sensors utilizing the FRET phenomenon.

For the first series of experiments (in Chapter 3), the α-pep F_1 antibody gave the largest change in responses as well as a small p-value. This antibody was selected to be examined further in the immobilization onto an optical fiber and in the gold nanoparticle system. Protein G was also selected for use in the subsequent immobilization experiments. In addition, the first series of experiments indicated that the use of the mycoplasma as the antigen produced a less variable biosensor response than the mycoplasma antigenic peptide does in similar systems. Also, the experiments in Chapter 3 concluded that the in-solution dose responses were not conducive to calibrated

responses. Though, it was shown that this biosensor detection system is able to detect very small concentrations with the ability to detect smaller concentrations with equally good responses.

The experiments performed in Chapter 4 demonstrated that the detection complexes did undergo conformational changes when silanized to the surface of the optical fiber, but the data were not statistically significant. In other words, the objective of developing a fiber optic biosensor to detect mycoplasmas was successful, but more experiments need to be performed in order to optimize A/D ratios and packing densities.

The Chapter 4 experiments also indicated that mycoplasma may be capable of exhibiting a lower detection limit than the peptides due to their stronger influence on conformational changes than the peptides. However, since these particular sensors are unable to give quantitative data, this sensor appears to be best suited as an early warning system to quickly and accurately detect the presence of *M. capricolum*.

Lastly, Chapter 5 examined a system involving gold nanoparticles. Gold nanoparticles are well known quenchers. This sensing technique should have provided good data on the conformational changes, but it failed to do so. Essentially, it was concluded that the parameters of this technique were not optimized. Further testing would need to be performed in order to conclude if this is a viable method for *M. capricolum* detection.

During the course of this research, a protocol for the future development of other specific mycoplasma sensors utilizing the FRET phenomenon was developed. Eventually, we want to fully develop this type of sensor so it can be used to accurately and quickly detect various pathogens for the Homeland Security Department.

REFERENCES

Abbas, A.K. and A.H. Lichtman. Cellular and Molecular Immunology. Fifth ed. 2003, Philadelphia, PA: SAUNDERS. 562.

Abel, A.P., M.G. Weller, G.L. Duveneck, M. Ehrat, and H.M.Widmer. Fiber Optic Evanescent Wave Biosensor for the Detection of Oligonucleotides. Analytical Chemistry, 1996. 68(17):2905-2912.

Ahmad, M. and L.L. Hench. Effect of Taper Geometries and Launch Angle on Evanescent Wave Penetration Depth in Optical Fibers. Biosensors and Bioelectronics, 2005. 20:1312-1319.

Alberts, B., A. Johnson, J. Lewis, M. Raff, K. Roberts, and P. Walter. Molecular Biology of the Cell. Fourth ed. 2002, New York, New York: Garland Science. 1463.

Al-Momani, W., M.A. Halablab, M.N. Abo-Shehada, K. Miles, L. McAuliffe, and R.A.J. Nicholas. Isolation and Molecular Identification of Small Ruminant Mycoplasmas in Jordan. Small Ruminant Research, 2005.

Baseman, J.B. and J.G. Tully. Mycoplasmas: Sophisticated, Reemerging, and Burdened by Their Notoriety. Emerging Infectious Diseases. 1997 Jan-Mar; 3(1):21-32.

Bhatia, S.K., L.C. Shriver-Lake, K.J. Prior, J.H. Georger, J.M. Calvert, R. Bredehorst, and F.S. Ligler. Use of Thiol-Terminal Silanes and Heterobifunctional Crosslinkers for Immobilization of Antibodies on Silica Surfaces. Anal Biochem, 1989. May 1;178(2):408-13.

Brecht, A., and G. Gauglitz. Optical probes and transducers. Biosensors and Bioelectronics, 1995. 10(9-10): p. 923-936.

Catterall, R.W. Chemical Sensors. 1997, Oxford, UK: Oxford University Press.

Chan, W.C., and S. Nie., Quantum dot bioconjugates for ultrasensitive nonisotopic detection. Science, 1998. 281(5385): p. 2016-2018.

Citti, C., G.F. Browning, and Renate Rosengarten. Phentypic Diversity and Cell Invastion in Host Subversion by Pathogenic Mycoplasmas. Mycoplasmas Molecular Biology Pathogenicity and Strategies for Control, Vol. 1. 2005: Horizon Bioscience.

Dubertret, B., M. Calame, and A.J. Libchaber. Single-mismatch detection using gold-quenched fluorescent oligonucleotides. Nature Biotechnology, 2001. 19:365-370.

Dulkeith, E., A.C. Morteani, T. Niedereichholz, T.A. Klar, and J. Feldmann., Fluorescence Quenching of Dye Molecules Near Gold Nanoparticles: Radiative and Nonradiative Effects. Physical Review Letters, 2002. 89(20).

Eggins, B.R., Chemical Sensors and Biosensors. Analytical Techniques in the Sciences, ed. D.J. Ando. 2002, Northern Ireland, UK: John Wiley & Sons, LTD. 273.

Fan, C., S. Wang, J.W. Hong, G.C. Bazan, K.W. Plaxco, and A.J. Heeger., Beyond superquenching: Hyper-efficient energy transfer from conjugated polymers to gold nanoparticles. Applied Physical Sciences, 2003. 100(11):6297-6301.

Frederix, F., K. Bonroy, W. Laureyn, G. Reekmans, A. Campitelli, W. Dehaen, and G. Maes., Enhanced Performance of an Affinity Biosensor Interface Based on Mixed Self-Assembled Monolayers of Thiols on Gold. Langmuir, 2003. 19:4351-4357.

Grant, S.A., D.J. Lichlyter, M.E. Pierce, L. Boettcher, and O. Soykan. Investigation of a FRET Immunosensor Technique for the Detection of Cardiac Troponin T and I. Sensor Letters, 5 January 2004. 2(1):58-63.

Grimm, J., J.M. Perez, L. Josephson and R. Weissleder. Novel Nanosensors for Rapid Analysis of Telomerase Activity. Cancer Research, 2004. 64:639-643.

Houshaymi, B., T. Tekleghiorghis, D.R. Worth, R.J. Miles, and R.A.J. Nicholas, Studies on Strains of Mycoplasma capricolum subsp. capripneumoniae Isolated from Outbreaks of Contagious Caprine Pleuropneumonia in Eritrea. Small Ruminant Research, 2002. 45(2):139-143.

Hu, Y. and G.S. Wilson. Rapid Changes in Local Extracellular Rat Brain Glucose Observed with an In Vivo Glucose Sensor. Journal of Neurochemistry, 1997 Apr; 68:1745-1752.

Ikheloa, J.O., A.T.P. Ajuwape, and A.I. Adetosoye, Biochemical Characterization and Serological Identification of Mycoplasmas Isolated from Pneumonic Lungs of Goats Slaughtered in Abattoirs in Northern Nigeria. Small Ruminant Research, 2003. 52(1-2): 93-97.

Ko, S. and S.A. Grant. Development of a novel FRET method for detection of Listeria or Salmonella. Sensors and Actuators, 2003. B(96):372-378.

Ko, S. and S.A. Grant. Development of a Novel FRET Immunosensor for Detection of Listeria. IEEE, 2003:288-292.

Koo, Y.-E.L., Y. Cao, R. Kopelman, S.M. Koo, M. Brasuel, and M.A. Philbert. Real-Time Measurement of Dissolved Oxygen Inside Live Cells by Organically Modified Silicate Fluorescent Nanosensors. Analytical Chemistry, 2004. 76(9):2498-2505.

Kurzawa, C., A. Hengstenberg, and W. Schuhmann. Immobilization Method for the Preparation of Biosensors Based on pH Shift-Induced Deposition of Biomolecule-Containing Polymer Films. Analytical Chemistry, 2002. 74(2):355-361.

Kusiluka, L.J.M., B. Ojeniyi, N.F. Friis, B. Kokotovic and P. Ahrens, Molecular Analysis of Field Strains of Mycoplasma capricolum subspecies capripneumoniae and Mycoplasma mycoides subspecies mycoides, Small Colony Type Isolated from Goats in Tanzania. Veterinary Microbiology, 2001. 82(1):27-37.

Lackowicz, J.R. Principles of Fluorescence Spectroscopy. Second ed. Vol. 1. 1999, New York, New York: Kulwer Academic/Plenum Publishers. 698.

Lichlyter, D.J., S.A. Grant, and O. Soykan. Development of a novel FRET immunosensor technique. Biosensors and Bioelectronics, 2003 Nov 30; 19(3):219-226.

Lieto, A.M., R.C. Cush, and N.L. Thompson. Ligand-Receptor Kinetics Measured by Total Internal Reflection with Fluorescence Correlation Spectroscopy. Biophysical Journal, 2003(85):3294-3302.

Liu, S. and H. Ju. Reagentless Glucose Biosensor Based on Direct Electron Transfer of Glucose Oxidase Immobilized on Colloidal Gold Modified Carbon Paste Electrode. Biosensors and Bioelectronics, 2003. 19:177-183.

Luo, X.-L., J.J. Xu, Y. Du, and H.Y. Chen. A Glucose Biosensor Based on Chitosan-Glucose Oxidase-Gold Nanoparticles Biocomposite Formed by One-Step Electrodeposition. Analytical Biochemistry, 2004. 334:284-289.

Mannelli, I., M. Minunni, S. Tombelli, and M. Mascini. Bulk Acoustic Wave Affinity Biosensor for Genetically Modified Organisms Detection. IEE Sensors Journal, 2003. 3(4):369-375.

Maran, A., C. Crepaldi, A. Tiengo, G. Grassi, E. Vitali, G. Pagano, S. Bistoni, . Calabrese, F. Santeusanio, F. Leonetti, M. Ribaudo, U. Di Mario, G. Annuzzi, S. Gensovese, G. Riccardi, M. Previti, D. Cucinotta, F. Giorgino, A. Bellomo, R. Giorgino, A. Poscia, and M. Varalli. Continuous Subcutaneous Glucose Monitoring in Diabetic Patients. Diabetes Care, 2002. 25(2):347-352.

Markham, P.F. and A.H. Noormohammadi. Diagnosis of Mycoplasmosis in Animals. Mycoplasmas Molecular Biology Pathogenicity and Strategies for Control. Vol 1. 2005: Horizon Bioscience.

Medintz, I.L., A.R. Clapp, H. Mattoussi, E.R. Goldman, B. Fisher, and J.M. Mauro. Self-Assembled Nanoscale Biosensors Based On Quantum Dot FRET Donors. Nature Materials, 2003. 2:630-638.

Mekler, V.M., A.Z. Averbakh, A.B. Sudarikov, and O.V. Kharitonova. Fluorescence energy transfer-sensitized photobleaching of a fluorescent label as a tool to study donor-acceptor distance distributions and dynamics in protein assemblies: studies of a complex of biotinylated IgM with streptavidin and aggregates of concanacalin A. Journal of Photochemistry and Photobiology, 1997. B(Biology 40):278-287.

Merriam-Webster's Collegiate Dictionary, 11th ed.

Nisman, R., G. Dellaire, Y. Ren, R. Li, and D.P. Bazett-Jones. Application of Quantum Dots as Probes for Correlative Fluorescence, Conventional, and Energy-filtered Transmission Electron Microscopy. Journal of Histochemistry and Cytochemistry, 2004. 52(1):13-18.

Olson, V.A., T. Laue, M.T. Laker, I.V. Babkin, C. Drosten, S.N. Shchelkunov, M. Niedrig, I.K. Damon, and H. Meyer. Real-Time PCR System for Detection of Orthopoxviruses and Simultaneous Identification of Smallpox Virus. Journal of Clinical Microbiology, 2004. 42(5):1940-1946.

Patolsky, F., G. Zheng, O. Hayden, M. Lakadamyali, X. Zhuang, and C.M. Liber. Electrical Detection of Single Viruses. PNAS, 2004. 101(39):14017-14022.

Pierce, M.E. and S.A. Grant. Development of a FRET Based Fiber-Optic Biosensor for Early Detection of Myocardial Infarction. Proceedings of the 26th Annual International Conference of the IEEE EMBS, 2004:2098-2101.

Rabbany, S.Y., B.L. Donner, and F.S. Ligler. Optical Immunosensors. Critical Reviews in Biomedical Engineering, 1994. 22(5/6):307-346.

Razin, S. Molecular biology and genetics of mycoplasmas (Mollicutes). Microbiol Rev 49:419, 1985.

Rottem, S. Interaction of Mycoplasmas with Host Cells. Physiological Reviews, 2003. 83:417-432.

Sapsford, K.E., Z. Liron, Y.S. Shubin, and F.S. Ligler. Kinetics of Antigen Binding to Arrays of Antibodies in Different Sized Spots. Analytical Chemistry, 2001. 73(22):5518-5524.

Sapsford, K.E., P.T. Charles, C.H. Patterson Jr., and F.S. Ligler. Demonstration of Four Immunoassay Formats Using the Array Biosensor. Analytical Chemistry, 2002. 74(5):1061-1068.

Schlecht, U., Y. Nomura, T. Bachmann, and I. Karube. Reversible Surface Thiol Immobilization of Carboxyl Group Containing Haptens to a BIAcore Biosensor Chip Enabling Repeated Usage of a Single Sensor Surface. Bioconjugate Chemistry, 2002. 13:188-193.

Schmid, J.A. and H.H. Sitte. Fluorescence resonance energy transfer in the study of cancer pathways. Current Opinion in Oncology, 2003. 15(1):55-64.
Serban, S. and N. El Murr. Use of Ferricinium Exchanged Zeolite for Mediator Stabilization and Analytical Performances Enhancement of Oxidase-Based Carbon Paste Sensors. Analytical Letters, 2003. 36(9):1739-1754.

Sharew, A.D., C. Staak, F. Thiaucourt, and F. Roger. A Serological Investigation into Contagious Caprine Pleuropneumonia (CCPP) in Ethiopia. Tropical Animal Health and Production, 2005. 37:11-19.

Taitt, C.R., U.S. Shubin, R. Angel, and F.S. Ligler. Detection of Salmonella enterica Serovar Typhimurium by Using a Rapid, Array-Based Immunosensor. Applied and Environmental Microbiology, 2004. Jan 2004:152-158.

Tolosa, L., H. Malak, G. Raob, and J.R. Lakowicz. Optical Assay for Glucose Based on the Luminescence Decay Time of the Long Wavelength Dye Cy5. Sensors and Actuators B, 1997. 45:93-99.

Unknown. Manual of Diagnostic Tests and Vaccines for Terrestrial Animals. 5th ed. 2005: OIE World Organization for Animal Health.

Dybvig, K. and L.L. Voelker. Molecular Biology of Mycoplasmas. Annual Review of Microbiology, 1996. 50:25-57.

Wagner, J.G., D.W. Schmidtke, C.P. Quinn, T.F. Fleming, B.Bernacky, and A. Heller. Continuous Amperometric Monitoring of Glucose in a Brittle Diabetic Chimpanzee with a Miniature Subcutaneous Electrode. Proc. Natl. Acad. Sci, 1998. 95:6379-6382.

Watzinger, F., M. Suda, S. Preuner, R. Baumgartinger, K. Ebner, L. Baskova, H.G.M. Niesters, A. Lawitschka, and T. Lion. Real-Time Quantitative PCR Assays for Detection and Monitoring of Pathogenic Human Viruses in Immunosuppressed Pediatric Patients. Journal of Clinical Microbiology, 2004. 42(11):5189-5198.

Wesonga, H.O, G. Bolske, F. Thiaucourt, C. Wanjohi, and R. Lindberg. Experimental Contagious Caprine Pleuropneumonia: A Long Term Study on the Course of Infection and Pathology in a Flock of Goats Infected with Mycoplasma capricolum subsp. capripneumoniae. Acta Veterinaria Scandinavica, 2004. 45(3-4):67-179.

Wise, K. Overview of mycoplasmas and reagents for sensor development. 2005: Columbia MO. Lab Meeting.

Wise, K., A. Madan, and M.J. Calcutt. Phase variable surface antigens confer strain and clonal diversity in Mycoplasma capricolum and the Mycoplasma mycoides cluster of mycoplasmas. Abstr. 103rd Gen. Mtg. American Society of Microbiology, 2003:296 (G-002).

Wolfe, D.B., R.S. Conroy, P. Garstecki, B.T. Mayers, M.A. Fischback, K.E. Paul, M. Prentiss, and G.M. Whitesides. Dynamic Control of Liquid-Core/ Liquid Cladding Optical Waveguides. Proceedings of the National Academy of Sciences of the United States of Americas, 2004. 101(34):12434-12438.

Woubit, S., S. Lorenzon, A. Peyraud, L. Manso-Silvan, and F. Thiaucourt. A Specific PCR for the Identification of Mycoplasma capricolum subsp. capripneumoniae, the Causative Agent of Contagious Caprine Pleuroneumonia. Veterinary Microbiology, 2004. 104(1-2):125-132.